

Millennial variations of atmospheric CO₂ during the early Holocene (11.7–7.4 ka)

Jinhwa Shin^{1,a}, Jinho Ahn¹, Jai Chowdhry Beeman², Hun-Gyu Lee¹, Jaemyeong Mango Seo³, and Edward J. Brook⁴

- 5 ¹School of Earth and Environmental Sciences, Seoul National University, Seoul, 151-742, Republic of Korea
²Laboratoire des Sciences du Climat et de l'Environnement, LSCE/IPSL, CEA-CNRS-UVSQ, Université Paris-Saclay, 91191, Gif-sur-Yvette, France
³Max-Planck Institute for Meteorology, Hamburg, 20146, Germany.
⁴College of Earth, Oceanic, and Atmospheric Sciences, Oregon State University, Corvallis, OR 97331-5506, U.S.A.
- 10 ^acurrent address: Department of Earth and Atmospheric Sciences, University of Alberta, Edmonton, AB, T6G 2E3, Canada

Correspondence to: Jinho Ahn (jinhoahn@snu.ac.kr)

Abstract. We present a new high-resolution record of atmospheric CO₂ from the Siple Dome ice core, Antarctica over the early Holocene (11.7–7.4 ka) that quantifies natural CO₂ variability on millennial timescales under interglacial climate conditions. Atmospheric CO₂ decreased by ~10 ppm between 11.3 and 7.3 ka. The decrease was punctuated by local minima at 11.1, 10.1, 9.1 and 8.3 ka with amplitude of 2–46 ppm. ~~Although the explanations of carbon cycle mechanisms remains uncertain due to insufficient paleoclimate records and model simulations,~~ These variations correlate with proxies for solar forcing and local climate in the South East Atlantic polar front, East Equatorial Pacific and North Atlantic. ~~These relationships suggest that weak solar forcing changes might have impacted CO₂ by changing CO₂ outgassing from the Southern Ocean and the East Equatorial Pacific and terrestrial carbon storage in the Northern Hemisphere over the early Holocene.~~ However, ~~However, the explanations of carbon cycle mechanisms linkage between atmospheric CO₂ and the climate change remains uncertain due to insufficient paleoclimate records and model simulations.~~ Additional CO₂ measurements from a higher accumulation site using better-quality ice cores and carbon cycle mechanistic models are needed to confirm the observation. studies using more precise methods and perhaps better quality ice cores.

15
20

1 Introduction

25 Future climate and ecosystem changes due to the continual increase of atmospheric carbon dioxide concentrations caused by human activities are inevitable (IPCC, 2013). Understanding the links between the carbon cycle and climate become important for accurate projection of future climate change. Atmospheric CO₂ is controlled by carbon exchange with ocean and land reservoirs, and increased CO₂ in the future and consequent changes in the earth system will in turn impact CO₂ levels via feedbacks (Friedlingstein et al., 2006). Due to the limited duration of direct measurements of atmospheric CO₂, which only
30 started in 1957 (Keeling, 1960), our understanding of the carbon cycle dynamics is limited on longer time scales. Air bubbles occluded in Antarctic ice cores allow us to reconstruct ancient air and may help us better understand the mechanisms that

control atmospheric CO₂ (Ahn and Brook, 2008, 2014; Bereiter et al., 2012; Higgins et al., 2015; Lüthi et al., 2008; Marcott et al., 2014; Nehrbass-Ahles et al., 2020; Petit et al., 1999).

35 Understanding the carbon cycle during interglacial periods is particularly useful because climate boundary conditions are similar to those of the near future. Previous work on late Holocene CO₂ records shows centennial CO₂ variability linked with climate, but the control mechanisms remain unclear, in part due to the potential mixture of natural and anthropogenic sources and sinks (Ahn et al., 2012; Bauska et al., 2015; Etheridge et al., 1996; Goosse, 2010; Indermühle et al., 1999; Rubino et al., 2013; Ruddiman, 2003, 2007). By contrast, CO₂ records for the early Holocene (11.7 to 7.3 ka) should reflect only natural CO₂ variability due to a smaller human population (Ruddiman, 2003).

40 The early Holocene (11.7–7.0 ka), is known as a relatively stable period in comparison with glacial periods. Several authors have linked centennial to millennial variability in the early Holocene to changes in solar forcing, including studies of the eastern equatorial Pacific (Marchitto et al., 2010), North Atlantic (Bond et al., 2001) and the Southern Ocean (Nielsen et al., 2004) with responses in proxy records at ~11.1, 10.1, 9.1 and 8.3 ka linked to solar variability (Bond et al., 2001; Marchitto et al., 2010). A weaker (stronger) solar activity has been linked with increased (decreased) ice-rafted debris in North Atlantic
45 (Bond cycle), dominant El-Niño-like conditions (La Niña-like conditions) in the eastern equatorial Pacific, weaker (stronger) Asian monsoons, expansion (reduction) of sea ice in the Southern Ocean and colder (warmer) sea surface temperature in the Southern Ocean (Bond et al., 2001; Marchitto et al., 2010; Nielsen et al., 2004; Reimer et al., 2004; Vonmoos et al., 2006). However, it is not clear what mechanisms are involved (Bond et al., 2001; Darby et al., 2012; Marchitto et al., 2010).

50 Atmospheric CO₂ on millennial time scales is mainly controlled by exchange with oceanic reservoirs and terrestrial carbon stocks. Existing atmospheric CO₂ records from EPICA Dome C (Dome C) show little variability of atmospheric CO₂ on millennial time scales from 10.9 to 7.3 ka (Monnin et al., 2001; Monnin et al., 2004). However, high-frequency signals might be muted due to gas trapping processes at this low-accumulation site (Spahni et al., 2003).

In this study, we measured 99 samples of atmospheric CO₂ with ages between 11.7 and 9.0 ka from the Siple Dome ice core. This new record complements the existing Siple Dome CO₂ record for 9.0–7.3 ka (Ahn et al., 2014). With this record, we
55 investigate the relationship between atmospheric CO₂ and climate variations on centennial and millennial time scales. Siple Dome benefits from an accumulation rate 4.2 times higher than at EDC and 1.8 times higher than at Taylor Dome (Table 1). A conservative estimate for the width of the gas age distribution in the Siple Dome record gives ~42 yrs for the early Holocene (Ahn et al., 2014). Thus, the Siple Dome ice core allows high temporal resolution and higher quality gas data with a more precise age scale and signals that are much less muted by the gas trapping process. The temporal resolution on average during
60 the early Holocene reaches ~30 yr as compared to ~80 yr in the EDC record.

2 Methods

2.1 CO₂ measurements

247 individual ice samples from 99 depth intervals were measured by needle cracker dry extraction and gas chromatography methods at Seoul National University (SNU) (see Figure S1 in SI (Supplementary Information)). We adopted the well-established measurement methods from Oregon State University (OSU) (Ahn et al., 2009) with minor modifications including sharpening of the tips of ice-crushing pins to increase the gas extraction efficiency, and use of a newer model Agilent 7890 gas chromatograph (GC).

Briefly, ice samples were cut and trimmed carefully with a band saw in a -21°C walk-in freezer at SNU. All visible cracks were removed to eliminate potential CO₂ alteration by trapping modern air. An ice sample of $\sim 8\text{--}10$ g was placed in a double walled vacuum chamber maintained at about -35°C using cold ethanol circulation between the walls of the chamber while flowing ultra-pure of N₂ gas (99.9999%) into the chamber. The ice sample was crushed in the cooled chamber by 91 steel needles moving straight up to down using a linear motion (bellows) vacuum feedthrough. The liberated air from the ice was collected for 3 min in a sample tube in a cryogenic system maintained at 11 K. The CO₂ mixing ratio was determined by the Agilent 7890A GC equipped with a flame-ionization detector, using a Ni catalyst which converts CO₂ to CH₄ before measurement. Sample air was injected into a stainless steel sample loop and the extracted air from each ice sample was analysed twice. The GC system was calibrated daily with a standard air tank (293.25 ppm CO₂, WMOX2007 mole fraction scale, calibrated by US National Oceanic and Atmospheric Administration, Global Monitoring Division). To examine the linearity of the GC, ice samples from five different depth intervals (CO₂ concentrations of 239–251 ppm) were analysed with two different air standards (188.9 and 293.3 ppm CO₂, respectively). The average difference in the results using the different standards was 0.4 ± 0.9 ppm (1σ) (Table S1 in SI).

2.2 Age scale of the Siple Dome ice core records

The Siple Dome samples are placed on the improved Siple Dome chronology developed by Yang et al. (2017), which is aligned with the Greenland Ice Core Chronology, 2005 (GICC05) using the synchronization of CH₄ and $\delta^{18}\text{O}_{\text{atm}}$ time series. Abrupt CH₄ changes have been shown to be synchronous within about 50 yrs with abrupt climate changes in Greenland during the last glacial period (Baumgartner et al., 2014; Rosen et al., 2014). Using this principle, abrupt changes in the composite Siple Dome CH₄ data were aligned with abrupt changes in $\delta^{18}\text{O}_{\text{ice}}$ from the NGRIP ice core (North Greenland Ice Core Project members, 2004; Rasmussen et al., 2006) at the 8.2 ka event and end of the Younger Dryas (Yang et al., 2017). For the time period of 11.64–8.10 ka, ages were updated from the original chronology of Severinghaus et al. (2009) by interpolating the age offsets at the tie points (Yang et al., 2017). For the time intervals outside of 11.64–8.10 ka, the age difference was set

90 constant with the difference at the closest tie point. The modified gas ages are younger than the Severinghaus et al. (2009) ages by less than ~110 yrs.

3 Results

3.1 The new high-resolution CO₂ record during the early Holocene

We obtained 99 data points that cover 622.14–539.06 m at SNU, corresponding to 11.7–9.0 ka (Figure 1). To extend the record to 7.4 ka, we made a composite dataset using a previous CO₂ record from the Siple Dome ice core covering 9.0–7.4 ka measured by the needle cracker system at OSU (Ahn et al., 2014) (Figure 1). Between 2 and 6 replicates (2.6 and 2.4 on average for SNU and OSU data, respectively) from individual depth intervals were analysed. The standard error of the mean of replicates from the same depth interval was 0.8 and 0.5 ppm on average for SNU and OSU data, respectively, ~~ranging from 0.01 to 1.75 ppm (1σ).~~ The sampling resolution is ~30 yrs for 11.7–9.0 ka and ~15 yrs for 9.0–7.3 ka.

To make a composite record of atmospheric CO₂, we tested for bias between the two data sets. Siple Dome samples from 7 depth intervals between 538.55–490.16 samples were analysed at both laboratories (Ahn et al., 2014). The SNU measurements were higher than the OSU measurements by 0.3±0.7 ppm (1σ) on average, indicating that the SNU and OSU results agree well (Table S2 in SI). The small offset of 0.3 ppm was added to OSU data before combining them with the SNU results.

3.2 Comparison with existing CO₂ records for the early Holocene

The new atmospheric CO₂ record from Siple Dome was compared to the existing CO₂ data from Dome C measured using the needle cracker at University of Bern (UB) (Monnin et al., 2001; Monnin et al., 2004) and the existing CO₂ data from the WAIS Divide ice core measured by the needle cracker at OSU (Marcott et al., 2014) (Figure 2A). On multi-millennial time scales, the baseline levels of the Siple Dome and WAIS Divide CO₂ records (Marcott et al., 2014) are higher than those from Dome C (Flückiger et al., 2002; Monnin et al., 2004) record (Figure 2A and Figure 2C). The CO₂ offset between the Dome C and Siple Dome ice cores is 3–6 ppm (Figure 2A and Figure 2C).

The offset between Siple Dome CO₂ data in this study and other CO₂ data sets could be related to differences in the analytical methods used to make the measurements. To examine the inter-laboratory analytical offset, several Taylor Dome ice samples were analysed at OSU (Ahn et al., 2014). The OSU results were higher than those at UB by 1.5 ppm on average. Taking the analytical offset between OSU and SNU of 0.3±0.7 ppm (1σ) into consideration, the 3–6 ppm CO₂ offset between the Siple Dome record (measured at OSU and SNU) and Dome C or Taylor Dome (measured at UB) cannot be entirely attributed to experimental offset.

To compare the new record to the existing records on millennial time scales, we calculate the Pearson correlation coefficient between Siple Dome CO₂ and existing CO₂ records. The offsets between existing CO₂ records and our data are also calculated (Figure 2). For these calculations, we use 250-yr running means of CO₂ records.

The Correlation coefficient between Siple Dome CO₂ and WAIS divide CO₂ is 0.7 ($p < 0.001$). However, the CO₂ offset between ~~WAIS divide-Dome C~~ record and Siple Dome record is quite random (~~Figure 2bA and 2C~~~~Figure 2B~~) because of scattering in the WAIS Divide CO₂ record during the early Holocene period. The WAIS Divide CO₂ data during the early Holocene was reconstructed from the ice just below the bubble clathrate transition zone (BTCZ). Previous studies raised an issue about the possibility of high frequency noise of atmospheric CO₂ record in the ice just below the BTCZ (Lüthi et al., 2010; Shackleton et al., 2019). This phenomenon might be related to gas fractionation effect because of clathrate layering during bubble-clathrate transformation. Gas content starts to be fractionated in the BCTZ because of the differential permeation of gas species when bubbles have transformed to clathrates. CO₂ concentration in the first layer of clathrates is more enriched with higher bubble-to-clathrate permeation rates. Below the BCTZ, gas content slowly homogenizes again through molecular diffusion (Bereiter et al., 2009), which can cause high frequency noise to the ice below the BCTZ. Thus, the WAIS Divide CO₂ data is not sufficient to discuss millennial variabilities of the early Holocene.

We observe that CO₂ data sets from Siple Dome and Dome C share similar trends in CO₂ variations despite the CO₂ offset in longer term means of 3–8 ppm. The CO₂ record from the Siple Dome is highly correlated with the CO₂ record from Dome C ($r = 0.89$, $p < 0.001$). The CO₂ offset between Dome C record and Siple Dome record decreases continuously from 11.7 ka to 7 ka with small variations at around 9.3 and 8.3 ka (Figure 2). The small variations of Dome C CO₂ record (1.4 ppm, compared to 3.0 ppm for Siple Dome) can be explained by the lower sampling resolution (~80 yrs for Dome C vs. ~20 yrs for Siple Dome) and a stronger damping effect on CO₂ concentration change at Dome C due to the slower gas trapping process at Dome C (Spahni et al., 2003).

The millennial CO₂ variations in the ice cores could be attributed to different degrees of in-situ ~~CO₂~~ production in ice. The in-situ production of CO₂ caused by carbonate-acid reactions (Anklin et al., 1997; Barnola et al., 1995; Delmas, 1993; Neftel et al., 1988; Smith et al., 1997a; Smith et al., 1997b) and oxidation of organic acids (Tschumi and Stauffer, 2000). Although Antarctic ice cores have relatively low concentrations of carbonates and lower site temperatures compared to Greenlandic ice cores (Tschumi and Stauffer, 2000), it is estimated that the in-situ production of CO₂ for Antarctic ice cores is smaller than 1.5 ppm (Bereiter et al., 2009). If the chemical alteration is the main cause of the millennial-scale CO₂ variations, we may expect to observe CO₂ age offsets among different cores because of dissimilar ice age-gas age differences. However, no available data set supports this possibility.

To further evaluate the in-situ CO₂ production, we considered potential reactions. First, we compared the CO₂ with non-sea-salt Ca (nssCa) content in the ice to check the carbonate-acid reaction in the ice. The concentration of nssCa is mainly controlled by dust delivery but it also can be produced partially by the carbonate-acid reaction in ice. Thus, we examined the concentration of nssCa ion in the Siple Dome and Dome C ice. The nssCa records do not correlate well with the filtered millennial CO₂ variations in both Siple Dome ($r = -0.33$) and Dome C ($r = 0.15$) records during the early Holocene (Figures S2 and Figure S3 in SI). In addition, the nssCa trends in Dome C and Siple Dome ice do not agree (Figures S2 and Figure S3 in SI), but millennial CO₂ variations do. Second, we checked the CO₂ production by oxidation of organic compounds (e.g., $2\text{H}_2\text{O}_2 + \text{HCHO} \rightarrow 3\text{H}_2\text{O} + \text{CO}_2$) in ice (Tschumi and Stauffer, 2000). The Dome C site is located further from the ocean than

155 Siple Dome and we therefore expect lower organic content in the Dome C ice. Concentrations of organic compounds at our
sampling depths are not available. However, the concentration of oxidant H₂O₂ on the top 2.5–100 m in the Siple Dome core
is below the detection limit of ~0.02 μM (McConnell, 1997), although 0.02 μM H₂O₂ still has potential to produce CO₂ and
can increase the mixing ratio in bubbles by 5 ppm given sufficient supply of organic compounds (Ahn et al., 2004).

In summary, the existing Dome C CO₂ record covering the early Holocene share similar trends in the Siple dome CO₂ record
160 despite an offset in longer term means of a few ppm. We note that CO₂ offsets of several ppm among different ice cores are
common features in different time intervals such as the last millennium (Ahn et al., 2012; Monnin et al., 2004; Rubino et al.,
2019; Siegenthaler et al., 2005) and Marine Isotope Stage 3 (Ahn et al., 2008; Bereiter et al., 2012) although they share the
same trends of CO₂ change on multi-centennial to multi-millennial time scales. Thus, it is likely that the millennial CO₂
variations during the early Holocene in the Siple Dome and Dome C cores reflect atmospheric CO₂ changes.

165 **3.3 Atmospheric CO₂ variations on the millennial time scale during the early Holocene**

Figure 1 shows the CO₂ record from Siple Dome during the early Holocene. CO₂ increased by ~8 ppm between 11.7 and 11.3
ka and then decreased by ~10 ppm from 10.9 to 7.3 ka. The rapid CO₂ increase at 11.7–11.3 ka might be associated with abrupt
warming in the North Atlantic and abrupt strengthening of Atlantic Meridional Overturning Circulation at the end of the last
glacial termination (Marcott et al., 2014; Monnin et al., 2001). The long term CO₂ trend is generally similar to that of the major
170 water isotope (δD) variations in Antarctic ice cores reflecting Antarctic temperature variations (Figure S4 in SI).

The Siple Dome CO₂ record shows millennial variability of ~2–~~4~~6 ppm with local minima at 11.1, 10.1, 9.1 and 8.3 ka (Figure
1). These variations resemble variability in other paleoclimate records that has been linked to solar cycle variations on these
time scales (Figures 3 and S5).

To examine the relationship between atmospheric CO₂ and the other paleoproxy data sets on millennial time scales, the Siple
175 Dome CO₂ record was smoothed and high pass filtered at 1/1800 yr due to two necessities. First, it is likely that high-frequency
variabilities of atmospheric CO₂ record (decadal-scale variations and centennial-scale variations) are high frequency noise of
atmospheric CO₂ record. Thus, we smoothed data sets to eliminate high-frequency variability. Before making a 250-yr running
mean, we made a 1-yr interpolation, because sample spacing between data points covering the early Holocene is not constant.
Second, to eliminate multi-millennial drift of CO₂ record, the data was high pass filtered at 1/1800 yr, following previous
180 methods by Bond et al. (2001) and Marchitto et al., (2010). The proxy records were also processed in the same way as the CO₂
record to remove high-frequency variability and long-term drift.

We evaluated uncertainties of the smoothed and high pass filtered CO₂ record using Monte Carlo simulation. Random sampling
was made from a probability distribution for each measured value and its standard deviation. We repeated this series of
simulations 10,000 times, which is shown as 2σ in Figure 1 (see SI for detailed information).

185 We calculated correlation coefficients between the filtered CO₂ and climate proxy series to understand their relationship with
atmospheric CO₂ (Figure 3, see SI for methods). To calculate correlation coefficients between records, we selected data from

11.45 ka to 7.45 ka. Correlation coefficients, their significance, and maximum correlation lags are shown in Figure 4 and Table 2. The CO₂ record from the Siple Dome is anti-correlated with the stacked IRD record in the North Atlantic (Bond et al., 2001) (r = -0.49 ± 0.1, CO₂ time lag of 120 ± 155 yrs), SST record in the eastern equatorial Pacific indicating El Niño-like or La Niña-like conditions (r = -0.41 ± 0.13, CO₂ time lag of 50 ± 219 yrs) (Marchitto et al., 2010), and sea ice in the Southern Ocean (r = -0.35 ± 0.17, CO₂ time lag of 190 ± 228 yrs) (Nielsen et al., 2004). On the other hand, the CO₂ record is positively correlated with summer sea-surface temperature (SSST) in the Southern Ocean (r = 0.35 ± 0.17, CO₂ time lag of 52 ± 228 yrs) (Nielsen et al., 2004). The results may imply a tentative link between atmospheric CO₂ variations and climate change on millennial time scales. The time lags might be caused by age uncertainties of the proxy records and/or response time of atmospheric CO₂ to climate change (Bauska et al., 2015; Bereiter et al., 2012; Carvalhais et al., 2014).

Interestingly, the highest anti-correlations we find are between the Siple Dome CO₂ record and the ¹⁴C production rate (r = -0.49 ± 0.12, CO₂ time lag of -20 ± 148 yrs) and ¹⁰Be flux (r = -0.52 ± 0.08, CO₂ time lag of 110 ± 63 yrs). This suggests that CO₂ and solar activity co-vary on millennial time scales (Figure 4 and Table 2). These observations imply that atmospheric CO₂ variations might be influenced by climate change driven by solar activity on millennial time scales during the early Holocene (11.7–7.0 ka) (Figure 4 and Table 2).

There are two outliers at ~11.08 and 10.8253 ka, which are far from the 250-running mean (Figure 1). Since the two outliers can enlarge the amplitude of actual CO₂ change, the data were processed except for the two values (Figures S7). The Siple Dome CO₂ record except for two data points at ~11.08 and 10.8253 ka was smoothed and high pass filtered at 1/1800 yr. With this processed data, we calculated correlation coefficients between the filtered CO₂ and climate proxy series again (Figure S6 and Table S3). The relationship between CO₂ data except for two outliers at ~11.08 and 10.8253 ka and climate proxies is similar to the relationship between original CO₂ record and climate proxies, which shows that two outliers do not highly impact our interpretation.

4 Discussion

4.1 Possible carbon cycle control mechanisms in the Early Holocene

Understanding a link between climate variations and solar activity on millennial time scales during the early Holocene is important to decipher carbon cycle mechanisms. However, the climate mechanisms have not yet been deciphered. A possible mechanism is that changes of solar activities may impact on stratospheric ozone concentrations, which can change stratospheric and tropospheric circulation patterns (Meehl et al., 2009). Higher solar activity may enhance the precipitation in the Intertropical Convergence Zone (ITCZ) and South Pacific Convergence Zone (SPCZ) (Meehl et al., 2009; van Loon et al., 2007). Consequently, the intensified moisture at those areas would increase trade wind strength and upwelling in the East Equatorial Pacific region. These conditions would lead to La Niña like climate states on millennial time scale (Marchitto et al., 2010). This change in the East Equatorial Pacific might have affected the North Atlantic (Darby et al., 2012).

If the CO₂ variations we observe are affected by solar variabilities via climate, a number of mechanisms could be involved, including the terrestrial or marine carbon cycles, or both. We discuss three possibilities here. First, a close relationship between CO₂ and climate proxies in Antarctica (Jouzel et al., 2007) on multi-millennial time scales (Figure S4) suggests that CO₂ variations on these time scales might be principally controlled by Southern Ocean processes. Atmospheric CO₂ can be controlled by temperature and salinity in the ocean (the solubility pump); solubility of CO₂ is greater in cooler and fresh surface waters (Broecker, 2002; Takahashi et al., 1993). The formation of deep water occurs in polar regions with high water density, where surface waters are cold, thus, the oceanic uptake of atmospheric CO₂ through this mechanism is stronger in polar regions (Sigman and Boyle, 2000). We observed a tentative link between atmospheric CO₂ and summer sea surface temperature (SSST) from the polar front region of the South East Atlantic on millennial time scales (Nielsen et al., 2004), which implies that lower SSST in the Southern Ocean might have lead to the reduction of atmospheric CO₂.

Increased sea ice extent might have blocked release of CO₂ from CO₂-rich deep water to the atmosphere, and therefore decreased atmospheric CO₂ concentration as previously suggested for glacial-interglacial CO₂ variations (Stephens and Keeling, 2000). Our Siple Dome CO₂ record is negatively correlated with the sea ice extent in the Southern Ocean, although the sea ice extent reconstruction shown in Figure 3 represents only the east Atlantic region of the Southern Ocean.

Oceanic processes associated with El Niño-like and La Niña-like climate variation could also impact the carbon cycle. Marine sediment cores from the East Equatorial Pacific show that solar activity proxies are well correlated with El Niño-like and La Niña-like climate variations in the East Equatorial Pacific SST proxy record (Marchitto et al., 2010). The East Equatorial Pacific is the region where CO₂-rich deep water upwells. Increased upwelling during La Niña -like conditions and resulting increased CO₂ outgassing have been suggested for the CO₂ increase during the last deglaciation (Kubota et al., 2014). Siple Dome CO₂ is anti-correlated with SST in the East Equatorial Pacific on millennial time scales (Figure 2), which may imply that La Niña-like climate can lead to higher CO₂ values.

Terrestrial carbon is involved with photosynthesis and respiration in plants, and with soil respiration (microbial and root respiration). Thus, terrestrial carbon is mostly controlled by temperature and precipitation (Davidson et al., 2000; Mielnick and Dugas, 2000). On multi-millennial time scales, when temperature in Greenland increases from 10.9 to 7.4 ka, atmospheric CO₂ decreases. Expansion of vegetation in the Northern Hemisphere may partially contribute to the decrease in atmospheric CO₂ (Indermühle et al., 1999).

A recent high resolution study for the last 1,200 yrs shows that centennial CO₂ variability was mainly controlled by terrestrial carbon, most likely in the high latitude of the Northern Hemisphere (Bauska et al., 2015). The stacked IRD from the North Atlantic may be used for an indicator of cool conditions in the North Atlantic (Bond et al., 1992; Bond et al., 2001). The strong relationship between IRD and atmospheric CO₂ indicates that colder climate in the North Atlantic may lower atmospheric CO₂ by impacting terrestrial carbon stocks during the early Holocene.

250 $\delta^{18}\text{O}_{\text{ice}}$ from the North Greenland Ice Core Project (NGRIP) ice core (Rasmussen et al., 2006) indicating temperature in Greenland also reveal millennial local minima at similar time intervals as those of CO_2 (~11.4, 10.9, 10.2, 9.3 and 8.2 ka), however, atmospheric CO_2 and temperature in Greenland are mismatched at the earliest early Holocene and ~8.2 ka. Thus, there is no significant linear relationship between CO_2 and temperature in Greenland on millennial time scales, and our calculation indicates that CO_2 leads temperature in Greenland on millennial time scales, though the correlation is still too small to assume any relationship ($r = 0.21 \pm 0.07$, CO_2 time lag of -130 ± 63 yrs).

255 Temperature in Greenland during the early Holocene might be partially influenced by the internal climate system or/and by low-latitude solar forcing indirectly. Two main cooling events in Greenland are recorded at ~11.4 and ~8.2 ka (Rasmussen et al., 2007). The well-known 8.2 ka cooling event is mainly influenced by the collapse of the Laurentide ice sheet (Merz et al., 2015) rather than by solar forcing; when temperature was colder in Greenland at ~11.4 ka, solar forcing was higher, not reaching a minimum at until ~11.2 ka. It is also elusive whether solar forcing has an influence on climate in Greenland at ~11.4 ka (Mekhaldi et al., 2020). In short, a linkage between atmospheric CO_2 and climate change during the early Holocene remains uncertain due to insufficient paleoclimate records and model simulations.

In this study, we observed that atmospheric CO_2 is highly correlated anti-correlated with the ^{14}C production rate and ^{10}Be flux with CO_2 time lag during the early Holocene (Figure 3). However it is the case that large variations of solar forcing at ~11.1, 10.1 and 8.3 ka. The ^{14}C production rate and ^{10}Be flux are correlated with CO_2 at ~9.1 ka on submillennial time scales.

265 We can also check the correlation of CO_2 with solar activity observe the similar phenomenon during during the last 2,000 years on centennial time scales (Figure S8)-. A positive correlation between solar forcing and atmospheric CO_2 is observed during the Little Ice Age (LIA). There are two periods in which sunspots were exceedingly rare. During the Maunder sunspot minimum (1647–1715 CE), total solar irradiance (TSI) was reduced by $0.85 \pm 0.16 \text{ W m}^{-2}$. Atmospheric CO_2 records from Antarctic ice cores commonly show a decrease trend during this period (Ahn et al., 2012; Monnin et al., 2004; Siegenthaler et al., 2005; Rubino et al., 2019). During the Spörer Minimum (1450–1550 CE), TSI record during this period also shows a decrease trend. However, atmospheric CO_2 decrease is not significant in Law Dome and EPICA Dronning Maud Land (EDML) records (Monnin et al., 2004; Siegenthaler et al., 2005; Rubino et al., 2019), while WAIS divide ice record shows a decrease during this period (Ahn et al., 2012) (Figure S87 in SI). However, Atmospheric CO_2 decrease drastically at ~1600 CE when - Total solar irradiance (TSI) shows a local maximum, which is similar to the relationship between solar forcing and atmospheric CO_2 at ~9.1 ka. To conclude, Atmospheric CO_2 concentration shows a local minimum. Thus, it is vague how solar forcing are related with atmospheric CO_2 variations on millennial time scales.

275 However, comparing the early and last Holocene requires attention due to different boundary conditions during these two periods and anthropogenic CO_2 during the late Holocene (e.g., Ruddiman, 2003, 2007). Variations of solar forcing are large on a centennial time scale during the Early Holocene. Thus, the solar output effect might be enhanced since the climate system is not responded linearly (Mohtadi et al., 2016). However, due to a decrease in summer insolation and the small variation of

280

~~solar forcing during the late Holocene (7–1 ka) (Berger, 1978), solar forcing might play a less important role during the late Holocene.~~

285 ~~Discussing the relationship between atmospheric CO₂ and solar forcing on shorter time scales during the late Holocene would be great to understand the major driver of millennial CO₂ variabilities during the early Holocene. However, further studies are needed to understand the relationship between atmospheric CO₂ and solar forcing on shorter time scales during the early Holocene with more proxy records and numerical models. Because since boundary conditions during the early Holocene and the late Holocene are different. Variations of solar forcing are large on a centennial time scale during the Early Holocene. Thus, the solar output effect might be enhanced since the climate system is not responded linearly (Mohtadi et al., 2016). However,~~
290 ~~due to a decrease in summer insolation and the small variation of solar forcing during the late Holocene (7–1 ka) (Berger, 1978), solar forcing might play a less important role during the late Holocene. However, further~~ Further studies are needed to understand the relationship between atmospheric CO₂ and solar forcing on shorter time scales during the early Holocene with more proxy records and numerical models.

5 Conclusion

295 In this study, we present a 30 yr-resolution CO₂ record during the early Holocene. Our data show that millennial atmospheric CO₂ variability of 2–46 ppm correlates with several climate proxies such as IRD in the North Atlantic, sea ice extent in the Southern Ocean, El Niño-like condition in the East Equatorial Pacific, all of which appear to coincidentally occur with solar activity minima (Bond et al., 2001; Marchitto et al., 2010; Nielsen et al., 2004; Reimer et al., 2004; Vonmoos et al., 2006). The relationships with the proxies are consistent with changes in several different mechanisms that could impact atmospheric
300 CO₂ on millennial time scales including changing CO₂ outgassing from the Southern Ocean and the East Equatorial Pacific, and changing terrestrial carbon storage in the Northern Hemisphere. Our new observations may improve our understanding of the relationship between interglacial climate and carbon cycles on millennial time scales in the absence of anthropogenic CO₂ perturbations. Further study should focus on clearly deciphering the millennial CO₂ control mechanisms with improved paleo proxy records and carbon cycle models.

305

Data availability. All data will be available on PANGAEA (Paleoclimatology database websites).

Author contributions. The research was designed by JS, JA and EB. The CO₂ measurements were performed by JS with contributions from HL and JA. The data analyses were led by JS and JCB with contributions from JMS and JA. JS wrote the
310 manuscript with inputs from all authors.

Competing interests. The authors declare that they have no conflict of interest.

Acknowledgements. Financial support was provided by Basic Science Research Program through the National Research Foundation of Korea (NRF) (NRF-2015R1A2A2A01003888; NRF-2020M1A5A1110607). This research was also partly conducted under US NSF grants (OPP 0944764 and ATM 0602395) to EB. Our special thanks go to Eunji Byun, Jisu Choi, Kyungmin Kim and Jiwoong Yang for analytical assistance, Youngcheol Han for data analyses. We also thank the staff of the National Ice Core Laboratory and Michael Kalk of Oregon State University for ice core curation and processing.

320

References

- Ahn, J. and Brook, E. J.: Siple Dome ice reveals two modes of millennial CO₂ change during the last ice age, *Nat. Commun.*, 5, 3723, <https://doi.org/10.1038/ncomms4723>, 2014.
- Ahn, J., Brook, E. J., and Buizert, C.: Response of atmospheric CO₂ to the abrupt cooling event 8200 years ago, *Geophys. Res. Lett.*, 41, 604–609, <https://doi.org/10.1002/2013gl058177>, 2014.
- Ahn, J., Brook, E. J., Mitchell, L., Rosen, J., McConnell, J. R., Taylor, K., Etheridge, D., and Rubino, M.: Atmospheric CO₂ over the last 1000 years: A high-resolution record from the West Antarctic Ice Sheet (WAIS) Divide ice core, *Global Biogeochem. Cy.*, 26, GB2027, <https://doi.org/10.1029/2011GB004247>, 2012.
- Ahn, J. H., Brook, E. J., and Howell, K.: A high-precision method for measurement of paleoatmospheric CO₂ in small polar ice samples, *J. Glaciol.*, 55, 499–506, 2009.
- Ahn, J. and Brook, E. J.: Atmospheric CO₂ and climate on millennial time scales during the last glacial period, *Science*, 322, 83–85, 2008.
- Ahn, J., Wahlen, M., Deck, B. L., Brook, E. J., Mayewski, P. A., Taylor, K. C., and White, J. W. C.: A record of atmospheric CO₂ during the last 40,000 years from the Siple Dome, Antarctica ice core, *J. Geophys. Res.*, 109, D13305, doi:10.1029/2003JD004415, 2004.
- Anklin, M., Schwander, J., Stauffer, B., Tschumi, J., Fuchs, A., Barnola, J-M., and Raynaud, D.: CO₂ record between 40 and 8 kyr B.P. from the Greenland Ice Core Project ice core, *J. Geophys. Res.*, 102, 26539–26545, 1997.
- Banta, J. R., McConnell, J. R., Frey, M. M., Bales, R.C., and Taylor, K.: Spatial and temporal variability in snow accumulation at the West Antarctic Ice Sheet Divide over recent centuries, *J. Geophys. Res.*, 113, D23102, <https://doi.org/10.1029/2008JD010235>, 2008.
- Barnola, J-M., Anklin, M., Porcheron, J., Raynaud, D., Schwander, J., and Stauffer, B.: CO₂ evolution during the last millennium as recorded by Antarctic and Greenland ice, *Tellus*, 47B, 264–272, <https://doi.org/10.3402/tellusb.v47i1-2.16046>, 1995.
- Baumgartner, M., Kindler, P., Eicher, O., Floch, G., Schilt, A., Schwander, J., Spahni, R., Capron, E., Chappellaz, J., Leuenberger, M., Fischer, H., and Stocker, T. F.: NGRIP CH₄ concentration from 120 to 10 kyr before present and its relation to a $\delta^{15}\text{N}$ temperature reconstruction from the same ice core, *Clim. Past*, 10, 903–920, doi:10.5194/cp-10-903-2014, 2014.
- Bauska, T. K., Joos, F., Mix, A. C., Roth, R., Ahn, J., and Brook, E. J.: Links between atmospheric carbon dioxide, the land carbon reservoir and climate over the past millennium, *Nat. Geosci.*, 8, 383–387, 2015.
- Bereiter, B., Lüthi, D., Siegrist, M., Schüpbach, S., Stocker, T. F., and Fischer, H.: Mode change of millennial CO₂ variability during the last glacial cycle associated with a bipolar marine carbon seesaw, *Proc. Natl. Acad. Sci.*, 109, 9755–9760, 2012.
- Bereiter, B., Schwander, J., Lüthi, D., and Stocker, T. F.: Change in CO₂ concentration and O₂/N₂ ratio in ice cores due to molecular diffusion, *Geophys. Res. Lett.*, 36, <https://doi.org/10.1029/2008GL036737>, 2009.

- Bond, G., Kromer, B., Beer, J., Muscheler, R., Evans, M. N., Showers, W., Hoffmann, S., Lotti-Bond, R., Hajdas, I., and Bonani, G.: Persistent solar influence on North Atlantic climate during the Holocene, *Science*, 294, 2130–2136, 2001.
- 355 Bond, G., Heinrich, H., Broecker, W., Labeyrie, L., McManus, J., Andrews, J., Huon, S., Jantschik, R., Clasen, S., Simet, C., Tedesco, K., Klas, M., Bonani, G., and Ivy, S.: Evidence for massive discharges of icebergs into the North Atlantic Ocean during the last glacial period, *Nature*, 360, 245–249, 1992.
- Broecker, W.: *The Glacial World According to Wally*, Eldigio Press, Palisades, New York. 346 pp, 2002.
- Carvalho, N., Forkel, M., Khomik, M., Bellarby, J., Jung, M., Migliavacca, M., Mu, M., Saatchi, S., Santoro, M., Thurner, 360 M., Weber, U., Ahrens, B., Beer, C., Cescatti, A., Randerson, J. T., and Reichstein, M.: Global covariation of carbon turnover times with climate in terrestrial ecosystems, *Nature*, 514, 213–217, <https://doi.org/10.1038/nature13731>, 2014.
- Darby, D. A., Ortiz, J., Grosch, C., and Lund, S.: 1,500-year cycle in the Arctic Oscillation identified in Holocene Arctic sea-ice drift, *Nat. Geosci.*, 5, 897–900, 2012.
- Davidson, E. A., Verchot, L. V., Cattanio, J. H., Ackerman, I. L., and Carvalho, J.: Effects of soil water content on soil 365 respiration in forests and cattle pastures of eastern Amazonia, *Biogeochemistry*, 48, 53–69, 2000.
- Delmas, R. J., A natural artefact in Greenland ice-core CO₂ measurements, *Tellus*, 45B (4), 391–396, <https://doi.org/10.1034/j.1600-0889.1993.t01-3-00006.x>, 1993.
- EPICA Dome C 2001 – 02 science and drilling teams: Extending the ice core record beyond half a million years, *Eos Trans. AGU*, AGU, 83(45), 509–517, 2002.
- 370 Etheridge, D. M., Steele, L., Langenfelds, R., Francey, R., Barnola, J. M., and Morgan, V.: Natural and anthropogenic changes in atmospheric CO₂ over the last 1000 years from air in Antarctic ice and firn, *J. Geophys. Res.*, 101, 4115–4128, 1996.
- Finkel, R. C. and Nishiizumi, K.: Beryllium 10 concentrations in the Greenland Ice Sheet Project 2 ice core from 3–40 ka, *J. Geophys. Res.*, 102(C12), 26699–26706, doi:199710.1029/97JC01282, 1997.
- Flückiger, J., Monnin, E., Stauffer, B., Schwander, J., Stocker, T. F., Chappellaz, J., Raynaud, D., and Barnola, J. M.: High 375 resolution Holocene N₂O ice core record and its relationship with CH₄ and CO₂, *Global Biogeochem. Cy.*, 16, 10-1–10-8, 2002.
- Friedlingstein, P., Bopp, L., Rayner, P., Betts, R., Jones, C., von Bloh, W., Brovkin, V., Cadule, P., Doney, S., Eby, M., Weaver, A. J., Fung, I., John, J., Joos, F., Strassmann, K., Kato, T., Kawamiya, M., and Yoshikawa, C.: Climate-carbon cycle feedback analysis: results from the C4MIP model intercomparison, *J. Climate*, 19, 3337–3353, 2006.
- 380 Goosse, H.: Degrees of climate feedback, *Nature*, 463, 438–439, doi:10.1038/463438a, 2010.
- Hamilton, G. S.: Mass balance and accumulation rate across Siple Dome, West Antarctica, *Ann. Glaciol.*, 35, 102–106, 2002.
- Higgins, J. A., Kurbatov, A. V., Spaulding, N. E., Brook, E., Introne, D. S., Chimiak, L. M., Yan, Y., Mayewski, P. A., and Bender, M. L.: Atmospheric composition 1 million years ago from blue ice in the Allan Hills, Antarctica, *P. Natl. Acad. Sci. USA*, 112, 6887–6891, <https://doi.org/10.1073/pnas.1420232112>, 2015.

- 385 Indermühle, A., Stocker, T. F., Joos, F., Fischer, H., Smith, H. J., Wahlen, M., Deck, B., Mastroianni, D., Tschumi, J., Blunier, T., Meyer, R., and Stauffer, B.: Holocene carbon-cycle dynamics based on CO₂ trapped in ice at Taylor Dome, Antarctica, *Nature*, 398, 121–126, 1999.
- IPCC, *Climate Change 2013: The Physical Science Basis. Contribution of Working Group I to the Fifth Assessment Report of the Intergovernmental Panel on Climate Change*, edited by: Stocker, T. F., Qin, D., Plattner, G. K., Tignor, M., Allen, S. K.,
- 390 Boschung, J., Nauels, A., Xia, Y., Bex, V., and Midgley, P. M., Cambridge University Press, Cambridge, United Kingdom and New York, NY, USA, 2013
- Jouzel, J., Masson-Delmotte, V., Cattani, O., Dreyfus, G., Falourd, S., Hoffmann, G., Minster, B., Nouet, J., Barnola, J. M., Chappellaz, J., Fischer, H., Gallet, J. C., Johnsen, S., Leuenberger, M., Loulergue, L., Luethi, D., Oerter, H., Parrenin, F., Raisbeck, G., Raynaud, D., Schilt, A., Schwander, A., Selmo, E., Souchez, R., Spahni, R., Stauffer, B., Steffensen, J. P., Stenni,
- 395 B., Stocker, T.F., Tison, J. L., Werner, M., and Wolff, E. W.: Orbital and Millennial Antarctic Climate Variability over the Past 800,000 Years, *Science* 317, 793–796, <https://doi.org/10.1126/science.1141038>, 2007.
- Keeling, C. D.: The concentration and isotopic abundances of carbon dioxide in the atmosphere, *Tellus*, 12, 200–203, <https://doi.org/10.3402/tellusa.v12i2.9366>, 1960.
- Kubota, K., Yokoyama, Y., Ishikawa, T., Obrochta, S., and Suzuki, A.: Larger CO₂ source at the equatorial Pacific during the
- 400 last deglaciation, *Sci. Rep.*, 4, <https://doi.org/10.1038/srep05261>, 2014.
- Lüthi, D., Le Floch, M., Bereiter, B., Blunier, T., Barnola, J.-M., Siegenthaler, U., Raynaud, D., Jouzel, J., Fischer, H., Kawamura, K., and Stocker, T. F.: High-resolution carbon dioxide concentration record 650,000–800,000 years before present, *Nature*, 453, 379–382, <https://doi.org/10.1038/nature06949>, 2008.
- Marchitto, T. M., Muscheler, R., Ortiz, J. D., Carriquiry, J. D., and van Geen, A.: Dynamical response of the tropical Pacific
- 405 Ocean to solar forcing during the early Holocene, *Science*, 330, 1378–1381, 2010.
- Marcott, S. A., Bauska, T. K., Buizert, C., Steig, E. J., Rosen, J. L., Cuffey, K. M., Fudge, T. J., Severinghaus, J. P., Ahn, J., Kalk, M. L., McConnell, J. R., Sowers, T., Taylor, K. C., White, J. W. C., and Brook, E. J.: Centennial-scale changes in the global carbon cycle during the last deglaciation, *Nature*, 514, 616–619, 2014.
- McConnell, J. R.: Investigation of the atmosphere-snow transfer process for hydrogen peroxide, Ph.D. dissertation, Univ. of
- 410 Ariz., Tucson, 1997.
- Meehl, G. A., Arblaster, J. M., Matthes, K., Sassi, F., and van Loon, H.: Amplifying the Pacific Climate System response to a small 11-year Solar Cycle forcing, *Science*, 325, 1114–1118, [doi:10.1026/science.1172872](https://doi.org/10.1026/science.1172872), 2009.
- Mekhaldi, F., Czymzik, M., Adolphi, F., Sjolte, J., Björck, S., Aldahan, A., Brauer, A., Martin-Puertas, C., Possnert, G., and Muscheler, R.: Radionuclide wiggle matching reveals a nonsynchronous early Holocene climate oscillation in Greenland and
- 415 western Europe around a grand solar minimum, *Clim. Past*, 16, 1145–1157, <https://doi.org/10.5194/cp-16-1145-2020>, 2020.
- Merz, N., Raible, C. C., and Woollings, T.: North Atlantic Eddy-Driven Jet in Interglacial and Glacial Winter Climates, *J. Climate*, 28, 3977–3997, <https://doi.org/10.1175/JCLI-D-14-00525.1>, 2015.

- Mielnick, P. C. and Dugas, W. A.: Soil CO₂ flux in a tallgrass prairie, *Soil Biol. Biochem.*, 32, 221–228, 2000.
- Monnin, E., Steig, E. J., Siegenthaler, U., Kawamura, K., Schwander, J., Stauffer, B., Stocker, T. F., Morse, D. C., Barnola,
420 J.-M., Bellier, B., Raynaud, D., and Fischer, H.: Evidence for substantial accumulation rate variability in Antarctica during the
Holocene through synchronization of CO₂ in the Taylor Dome, Dome C and DML ice cores, *Earth Planet. Sc. Lett.*, 224, 45–
54, 2004.
- Monnin, E., Indermuhle, A., Dallenbach, A., Fluckiger, J., Stauffer, B., Stocker, T. F., Raynaud, D., and Barnola, J.-M.:
Atmospheric CO₂ concentrations over the last glacial termination, *Science*, 291(5501), 112–114, 2001.
- 425 Morse, D., Blankenship, D., Waddington, E., and Neumann, T.: A site for deep ice coring in West Antarctica: Results from
aerogeophysical surveys and thermal-kinematic modeling, *Ann. Glaciol.*, 35, 36–44, 2002.
- Mortyn, P. G., Charles, C. D., Ninnemann, U. S., Ludwig, K., and Hodell, D. A.: Deep sea sedimentary analogues for the
Vostok ice core, *Geochem. Geophys. Geosy.*, 4, 8405, doi:10.1029/2002GC000475, 2003.
- Neftel, A., Oeschger, H., Staffelbach, T., and Stauffer, B.: CO₂ record in the Byrd ice core 50,000–5,000 years bp, *Nature*,
430 331, 609–611, doi:10.1038/331609a0, 1988.
- Nehrbass-Ahles, C., Shin, J., Schmitt, J., Bereiter, B., Joos, F., Schilt, A., Schmidely, L., Silva, L., Teste, G., Grilli, R.,
Chappellaz, J., Hodell, D., Fischer, H., and Stocker, T. F.: Abrupt CO₂ release to the atmosphere under both glacial and early
interglacial conditions, *Science*, 369, 1000–1005, 2020.
- Nielsen, S. H. H., Koc, N., and Crosta, X.: Holocene climate in the Atlantic sector of the southern ocean: Controlled by
435 insolation or oceanic circulation?, *Geology*, 32, 317–320, 2004.
- North Greenland Ice Core Project members: High-resolution record of northern hemisphere climate extending into the last
interglacial period, *Nature*, 431, 147–151, 2004.
- Petit, J. R., Jouzel, J., Raynaud, D., Barkov, N. I., Barnola, J.-M., Basile, I., Bender, M., Chappellaz, J., Davis, M., Delaygue,
G., Delmotte, M., Kotlyakov, V. M., Legrand, M., Lipenkov, V.Y., Lorius, C., Pepin, L., Ritz, C., Saltzman, E., and
440 Stievenard, M.: Climate and atmospheric history of the past 420,000 years from the Vostok ice core, Antarctica, *Nature*, 399,
429–436, <https://doi.org/10.1038/20859>, 1999.
- Rasmussen, S. O., Vinther, B. M., Clausen, H. B., and Andersen, K. K.: Early Holocene climate oscillations recorded in three
Greenland ice cores, *Quat. Sci. Rev.*, 26, 1907–1914, 2007.
- Rasmussen, S. O., Andersen, K. K., Svensson, A. M., Steffensen, J. P., Vinther, B. M., Clausen, H. B., Siggaard-Andersen,
445 M.-L., Johnsen, S. J., Larsen, L. B., Dahl-Jensen, D., Bigler, M., Rothlisberger, R., Fischer, H., Goto-Azuma, K., Hansson,
M.E., and Ruth, U.: A new Greenland ice core chronology for the last glacial termination, *J. Geophys. Res.*, 111, D06102,
<https://doi.org/10.1029/2005JD006079>, 2006.
- Reimer, P. J., Baillie, M. G. L., Bard, E., Bayliss, A., Beck, J. W., Blackwell, P. G., Bronk Ramsey, C., Buck, C. E., Burr, G.
S., Edwards, R. L., Friedrich, M., Grootes, P. M., Guilderson, T. P., Hajdas, I., Heaton, T. J., Hogg, A. G., Hughen, K. A.,
450 Kaiser, K. F., Kromer, B., McCormac, F. G., Manning, S. W., Reimer, R. W., Richards, D. A., Southon, J. R., Talamo, S.,

- Turney, C. S. M., van der Plicht, J., and Weyhenmeyer, C. E.: IntCal09 and Marine09 radiocarbon age calibration curves, 0–50,000 years cal BP, *Radiocarbon*, 51, 1111–1150, 2009.
- Reimer, P. J., Baillie, M. G., Bard, E., Beck, J. W., Buck, C. E., Blackwell, P. G., Burr, G. S., Cutler, K. B., Damon, P. E., Edwards, R. L., Fairbanks, R. G., Friedrich, M., Guilderson, T. P., Hogg, A. G., Hughen, K. A., Kromer, B., McCormac, G., Ramsey, C. B., Reimer, R. W., Remmele, S., Southon, J. R., Stuvier, M., Taylor, F. W., van der Plicht, J., and Weyhenmeyer, C. E.: IntCal04: A New Consensus Radiocarbon Calibration Dataset from 0–26 ka BP, *Radiocarbon*, 46, 1029–1058, 2004.
- 455 Rosen, J. L., Brook, E. J., Severinghaus, J. P., Blunier, T., Mitchell, L. E., Lee, J. E., Edwards, J. S., and Gkinis, V.: An ice core record of near-synchronous global climate changes at the Bølling transition, *Nat. Geosci.*, 7, 459–463, 2014.
- Rubino, M., Etheridge, D. M., Thornton, D. P., Howden, R., Allison, C. E., Francey, R. J., Langenfelds, R. L., Steele, L. P., Trudinger, C. M., Spencer, D. A., Curran, M. A. J., van Ommen, T. D., and Smith, A. M.: Revised records of atmospheric trace gases CO₂, CH₄, N₂O, and δ¹³C-CO₂ over the last 2000 years from Law Dome, Antarctica, *Earth Syst. Sci. Data*, 11, 473–492, <https://doi.org/10.5194/essd-11-473-2019>, 2019.
- 460 Rubino, M., Etheridge, D. M., Trudinger, C. M., Allison, C. E., Battle, M. O., Langenfelds, R. L., Steele, L. P., Curran, M., Bender, M., White, J. W. C., Jenk, T. M., Blunier, T., and Francey, R. J.: A revised 1000 year atmospheric ¹³C-CO₂ record from Law Dome and South Pole, Antarctica, *J. Geophys. Res.*, 118, 8382–8499, doi:10.1002/jgrd.50668, 2013.
- 465 Ruddiman, W. F.: The early anthropogenic hypothesis: challenges and responses, *Rev. Geophys.*, 45, RG4001, doi:10.1029/2006RG000207, 2007.
- Ruddiman, W. F.: The anthropogenic greenhouse era began thousands of years ago, *Clim. Change*, 61, 261–293, doi:10.1023/B:CLIM.0000004577.17928.fa, 2003.
- 470 Schwander, J., Jouzel, J., Hammer, C. U., Petit, J.-R., Udisti, R., and Wolff, E.: A tentative chronology for the EPICA Dome Concordia ice core, *Geophys. Res. Lett.*, 28(22), 4243–4246, 2001.
- Severinghaus, J. P., Beaudette, R., Headly, M. A., Taylor, K., and Brook, E. J.: Oxygen-18 of O₂ records the impact of abrupt climate change on the terrestrial biosphere, *Science*, 324, 1431–1434, 2009.
- Severinghaus, J. P., Grachev, A., and Battle, M.: Thermal fractionation of air in polar firn by seasonal temperature gradients, *Geochem. Geophys. Geosyst.*, 2, 1048–1024, doi:10.1029/2000GC000146, 2001.
- 475 Shackleton, S., Bereiter, B., Baggenstos, D., Bauska, T. K., Brook, E. J., Marcott, S. A., and Severinghaus, J. P.: Is the Noble Gas-Based Rate of Ocean Warming During the Younger Dryas Overestimated?, *Geophys. Res. Lett.*, 46, 5928–5936, <https://doi.org/10.1029/2019GL082971>, 2019.
- Siegenthaler, U., Monnin, E., Kawamura, K., Spahni, R., Schwander, J., Stauffer, B., Stocker, T. F., Barnola, J.-M., and Fischer, H.: Supporting evidence from the EPICA Dronning Maud Land ice core for atmospheric CO₂ changes during the past millennium, *Tellus B*, 57(7), 51–57, doi:10.1111/j.1600-0889.2005.00131.x, 2005.
- 480 Sigman, D. M. and Boyle, E. A.: Glacial/interglacial variations in atmospheric carbon dioxide, *Nature*, 407, 859–869, <https://doi.org/10.1038/35038000>, 2000.

- Smith, H., Wahlen, M., Mastroianni, D., and Taylor, K.: The CO₂ concentration of air trapped in GISP2 ice from the Last
485 Glacial Maximum-Holocene transition, *Geophys. Res. Lett.*, 24, 1–4, <https://doi.org/10.1029/96GL03700>, 1997a.
- Smith, H., Wahlen, M., Mastroianni, D., Taylor, K., and Mayewski, P.: The CO₂ concentration of air trapped in Greenland Ice
Sheet Project 2 ice formed during periods of rapid climate change, *J. Geophys. Res.*, 102, 26577–26582,
<https://doi.org/10.1029/97JC00163>, 1997b.
- Spahni, R., Schwander, J., Fluckinger, J., Stauffer, B., Chapellaz, J., and Raynaud, D.: The attenuation of fast atmospheric
490 CH₄ variations recorded in polar ice cores, *Geophys. Res. Lett.*, 30, 1571, doi:10.1029/2003GL017093, 2003.
- Stephens, B. B. and Keeling, R. F.: The influence of Antarctic sea ice on glacial-interglacial CO₂ variations, *Nature*, 404, 171–
174, <https://doi.org/10.1038/35004556>, 2000.
- Tabacco, I. E., Passerini, A., Corbelli, F., and Gorman, M.: Determination of the surface and bed topography at Dome C, East
Antarctica, *J. Glaciol.*, 44, 185–191, 1998.
- 495 Takahashi, T., Olafsson, J., Goddard, J. G., Chipman, D. W., and Sutherland, S. C.: Seasonal variation of CO₂ and nutrients in
the high-latitude surface oceans: A comparative study, *Global Biogeochem. Cy.*, 7, 843–878,
<https://doi.org/10.1029/93GB02263>, 1993.
- Taylor, K. C., White, J. W. C., Severinghaus, J. P., Brook, E. J., Mayewski, P. A., Alley, R. B., Steig, E. J., Spencer, M. K.,
Meyerson, E., Meese, D. A., Lamorey, G. W., Grachev, A., Gow, A. J., and Barnett, B. A.: Abrupt climate change around 22
500 ka on the Siple Coast of Antarctica, *Quaternary Sci. Rev.*, 23, 7–15, doi:10.1016/j.quascirev.2003.09.004, 2004.
- Tschumi, J. and Stauffer, B.: Reconstructing past atmospheric CO₂ concentration based on ice-core analyses: open questions
due to in situ production of CO₂ in the ice, *J. Glaciol.*, 46, 45–53, 2000.
- van Loon, H., Meehl, G. A., and Shea, D. J., Coupled air-sea response to solar forcing in the Pacific region during northern
winter, *J. Geophys. Res.*, 112, D02108, doi:10.1029/2006JD007378, 2007.
- 505 Vonmoos, M., Beer, J., and Muscheler, R.: Large variations in Holocene solar activity: Constraints from ¹⁰Be in the Greenland
Ice Core Project ice core, *J. Geophys. Res.-Space*, 111, A10105, doi:10.1029/2005JA011500, 2006.
- Waddington, E. and Morse, D. L.: Spatial variations of local climate at Taylor Dome, Antarctica: Implications for paleoclimate
from ice cores., *Ann. Glaciol.*, 20, 219–225, <https://doi.org/10.3189/172756494794587014>, 1994.
- Yang, J.-W., Ahn, J., Brook, E. J., and Ryu, Y.: Atmospheric methane control mechanisms during the early Holocene, *Clim.*
510 *Past*, 13, 1227–1242, <https://doi.org/10.5194/cp-13-1227-2017>, 2017.

Table 1. Glaciological characteristics of Antarctic ice cores.

Core name	Mean Annual Temperature (°C)	Mean Accumulation Rate as Water Equivalent (g cm ⁻² yr ⁻¹ as water equivalent)	References
Siple Dome	-25.4	12.4	Hamilton (2002); Severinghaus et al. (2001); Taylor et al. (2004)
Taylor Dome	-42	7	Waddington and Morse (1994)
EPICA Dome C	-54	3	Schwander et al.(2001); EPICA Dome C 2001-02 Science and Teams (2002); Tabacco et al.(1998)
WAIS Divide	-31	20	Banta et al.(2008); Morse et al.(2002)

Table 2. Correlation between Siple Dome CO₂ record and climate proxy records. Column A shows correlation coefficients between CO₂ and proxies with CO₂ time lags. Column B shows correlation coefficients between CO₂ and proxies without CO₂ time lag. “With MC” are mean values from the simulations taking age uncertainties into account. “Without MC” is the classic calculation of correlation, without taking age uncertainty into account. Significance of the lag correlations was assessed against 1,000 repetitions of the lag correlation calculation using synthetic data stochastically generated to have the same red noise characteristics as the original series.

Proxy records (Reference)	A: Correlation between CO ₂ and proxies with CO ₂ time lag (yrs)				B: Correlation between CO ₂ and proxies without CO ₂ time lag	
	With MC		Without MC		With MC	Without MC
	r (p-value)	Time lag	r (p-value)	Time lag	r (p-value)	r (p-value)
CO ₂ - ¹⁴ C production rate Marchitto et al.(2010); Reimer et al.(2004)	-0.49± 0.12 (0.3192)	-20±148	- 0.76 (0.0003)	50	-0.48 (0.007)	-0.70 (< 0.001)
CO ₂ - ¹⁰ Be flux from Greenland ice core Finkel and Nishiizumi (1997); Marchitto et al. (2010); Vonmoos et al. (2006)	-0.52± 0.08 (0.2847)	110±63	- 0.61 (0.0087)	110	-0.29 (0.05)	-0.32 (< 0.001)
CO ₂ - IRD from the North Atlantic region Bond et al. (2001); Marchitto et al. (2010)	-0.49± 0.1 (0.3084)	120±155	- 0.73 (0.0009)	170	-0.33 (0.05)	-0.21 (< 0.001)
CO ₂ - SST from eastern equatorial Pacific Marchitto et al. (2010)	-0.40± 0.13 (0.337)	50±219	- 0.61 (0.009)	80	-0.38 (0.04)	-0.55 (< 0.001)
CO ₂ - Sea ice in the Southern Ocean Nielsen et al. (2004)	-0.35± 0.17 (0.2899)	190±228	- 0.57 (0.0151)	100	-0.24 (0.17)	-0.48 (< 0.001)
CO ₂ - SST in the Southern Ocean Nielsen et al. (2004)	0.35± 0.17 (0.3070)	52±228	0.57 (0.0144)	30	0.35 (0.06)	0.56 (< 0.001)
CO ₂ - NGRIP δ ¹⁸ O Rasmussen et al. (2006)	0.21± 0.07 (0.2684)	-130±63	0.11 (0.3411)	270	0.09 (0.5)	0.06 (0.2)

520

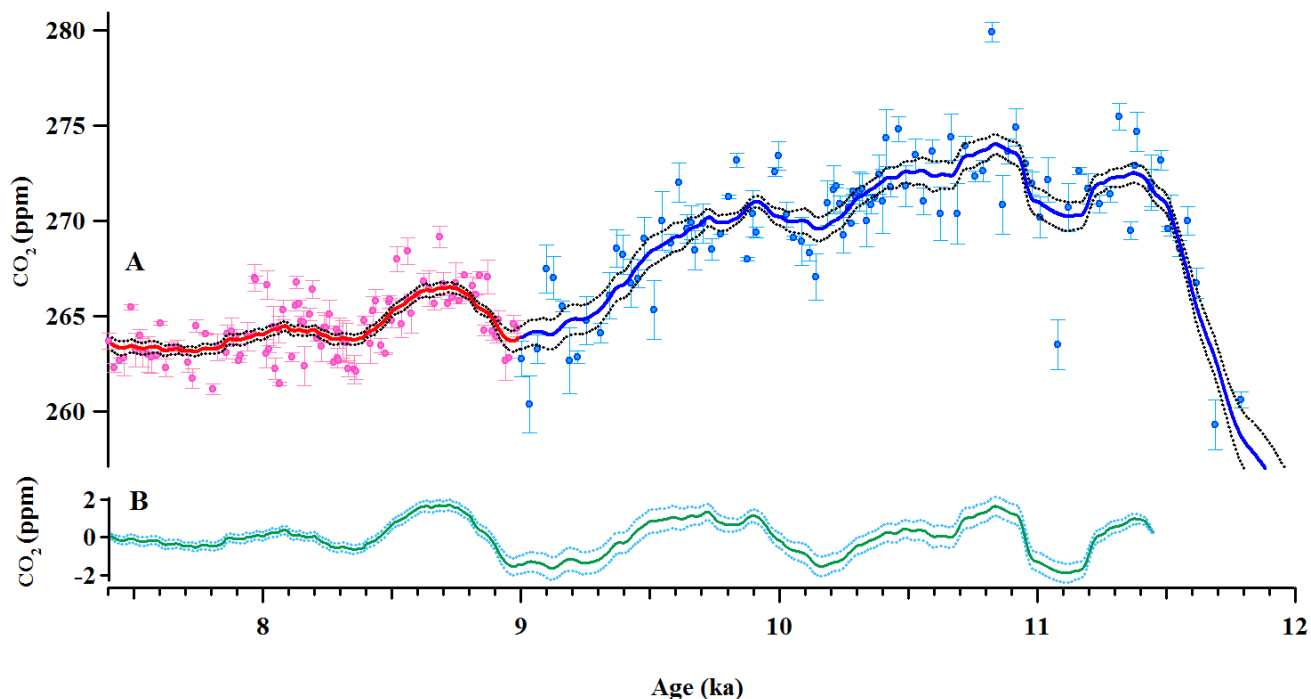


Figure 1. High-resolution atmospheric CO₂ records obtained from Siple Dome ice core, Antarctica during the early Holocene. A. Pink and blue circles are Siple Dome ice core records obtained at Oregon State University (Ahn et al., 2014) and Seoul National University (this study), respectively. Lines represent 250-yr running means and dotted lines, 2 σ uncertainties calculated from Monte Carlo simulation. For the simulation, we produced 10,000 different sets of CO₂ concentrations which vary randomly with Gaussian propagation in their uncertainties. B. Green line indicates 250-yr running means of the original Siple Dome CO₂ data processed by high-pass filtering at 1/1800 yr⁻¹. Blue line indicates ~~2 σ uncertainties of calculated from Monte Carlo simulation.~~ 2 σ uncertainties of the 250-year mean value, and cannot be used to interpret variations on shorter timescales.

525

530

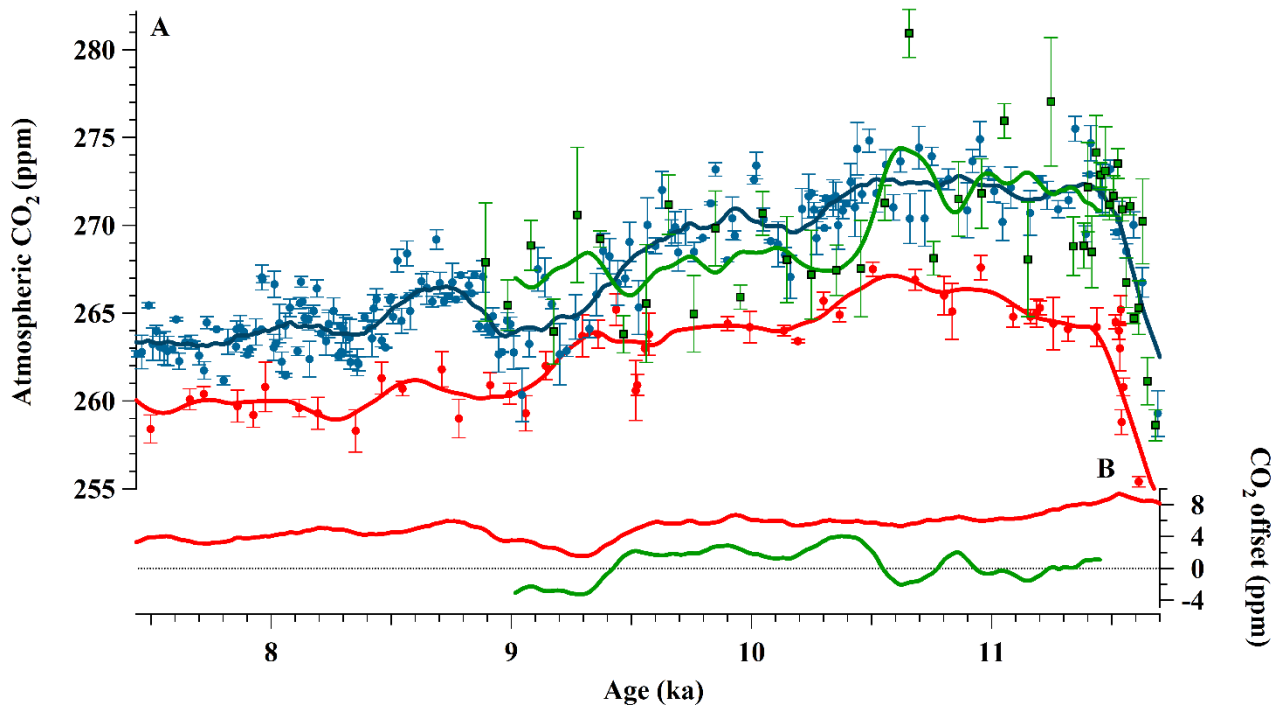
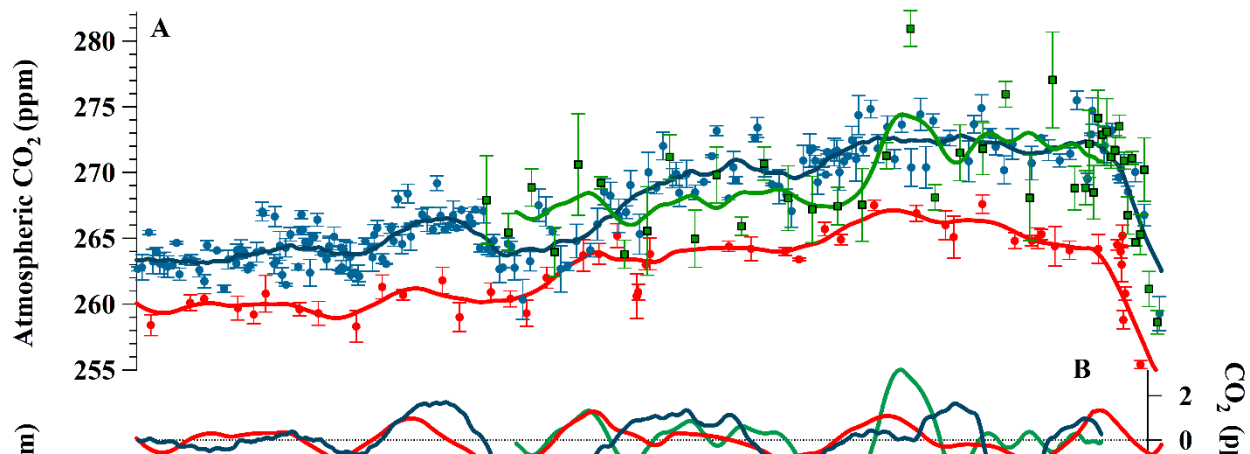


Figure 2. **A:** Atmospheric CO₂ records. Red dots: Atmospheric CO₂ record from Dome C ice core. Red line: 250-yr running means of atmospheric CO₂ record from Dome C ice core. Blue dots: Atmospheric CO₂ record from Siple Dome ice core. Blue line: 250-yr running means of atmospheric CO₂ record from Siple Dome ice core. Green dots: Atmospheric CO₂ record from WAIS Divide ice core. Green line: 250-yr running means of atmospheric CO₂ record from WAIS Divide ice core. **B:** Blue line indicates 250-yr running means of the original Siple Dome CO₂ data processed by high-pass filtering at 1/1800 yr⁻¹. Green line indicates 250-yr running means of the original WAIS Divide CO₂ data processed by high-pass filtering at 1/1800 yr⁻¹. Red line indicates 250-yr running means of the original WAIS Divide CO₂ data processed by high-pass filtering at 1/1800 yr⁻¹. **C,B:** CO₂ offset between Siple Dome CO₂ record and other published CO₂ records. Red line: CO₂ offset between Siple Dome CO₂ record and Dome C CO₂ record. Green line: CO₂ offset between Siple Dome CO₂ record and WAIS divide CO₂ record.



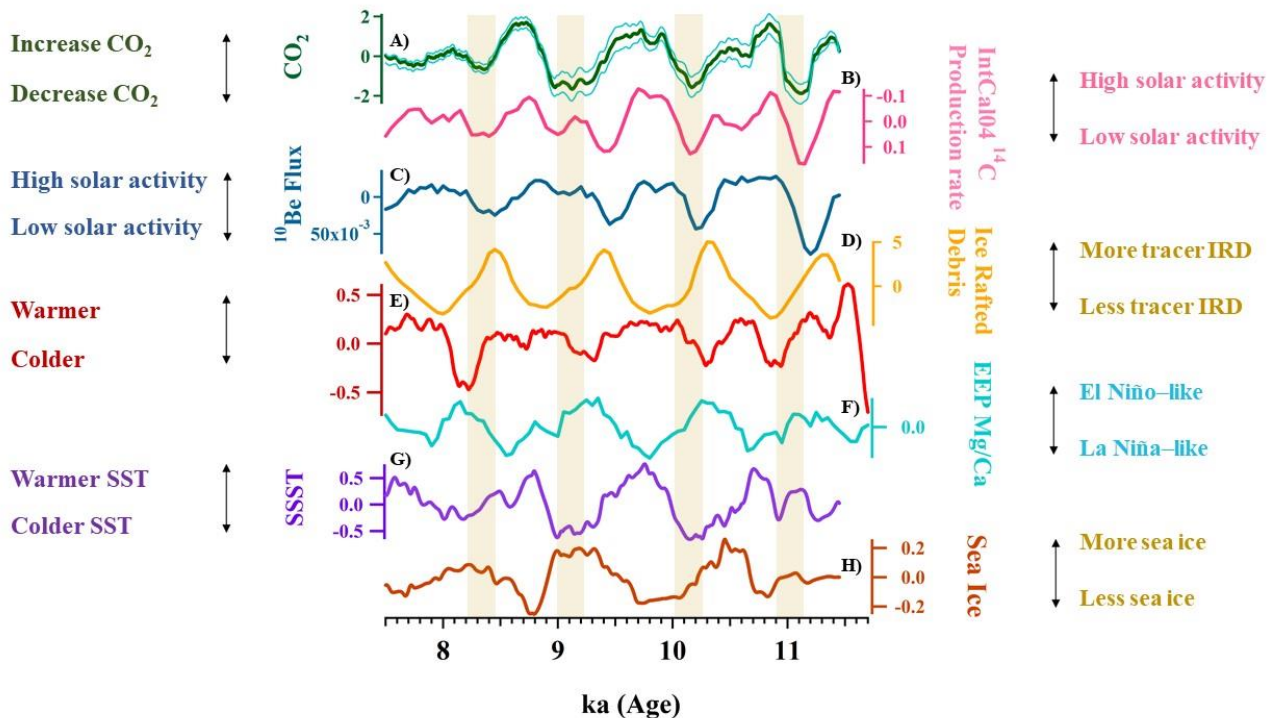


Figure 3. Comparison of atmospheric CO₂ with climatic proxy records over the early Holocene. The records were smoothed at ~250 yrs and high-pass filtered at 1/1800 yr⁻¹. A) Atmospheric CO₂ record from Siple Dome (in this study). Dotted lines, 2σ uncertainties calculated from Monte Carlo simulation. B) ¹⁴C production rate from IntCal04 Δ¹⁴C data (Marchitto et al., 2010; Reimer et al., 2004). C) ¹⁰Be flux record from ice core on the GICC05 timescale (Finkel and Nishiizumi, 1997; Marchitto et al., 2010; Rasmussen et al., 2006; Vonmoos et al., 2006). D). IRD stacked records from the North Atlantic regions on untuned calibrated ¹⁴C age model (Bond et al., 2001; Marchitto et al., 2010). E) North Greenland Ice Core Project (NGRIP) ice core isotope ratio on the GICC05 timescale (Rasmussen et al., 2006). F) Sea surface temperature from the eastern equatorial Pacific indicating El Niño-like or La Niña-like conditions (Marchitto et al., 2010). The data was radiocarbon dated by accelerator mass spectrometry (AMS), which was recalibrated by the Marine09 calibration curve (Reimer et al., 2009). G) Sea surface temperature from the Polar Front of the Southern Ocean on the chronology of Mortyn et al. (2003) (Nielsen et al., 2004). H) Sea ice presence from the Polar Front of the Southern Ocean on the chronology of Mortyn et al. (2003) (Nielsen et al., 2004).

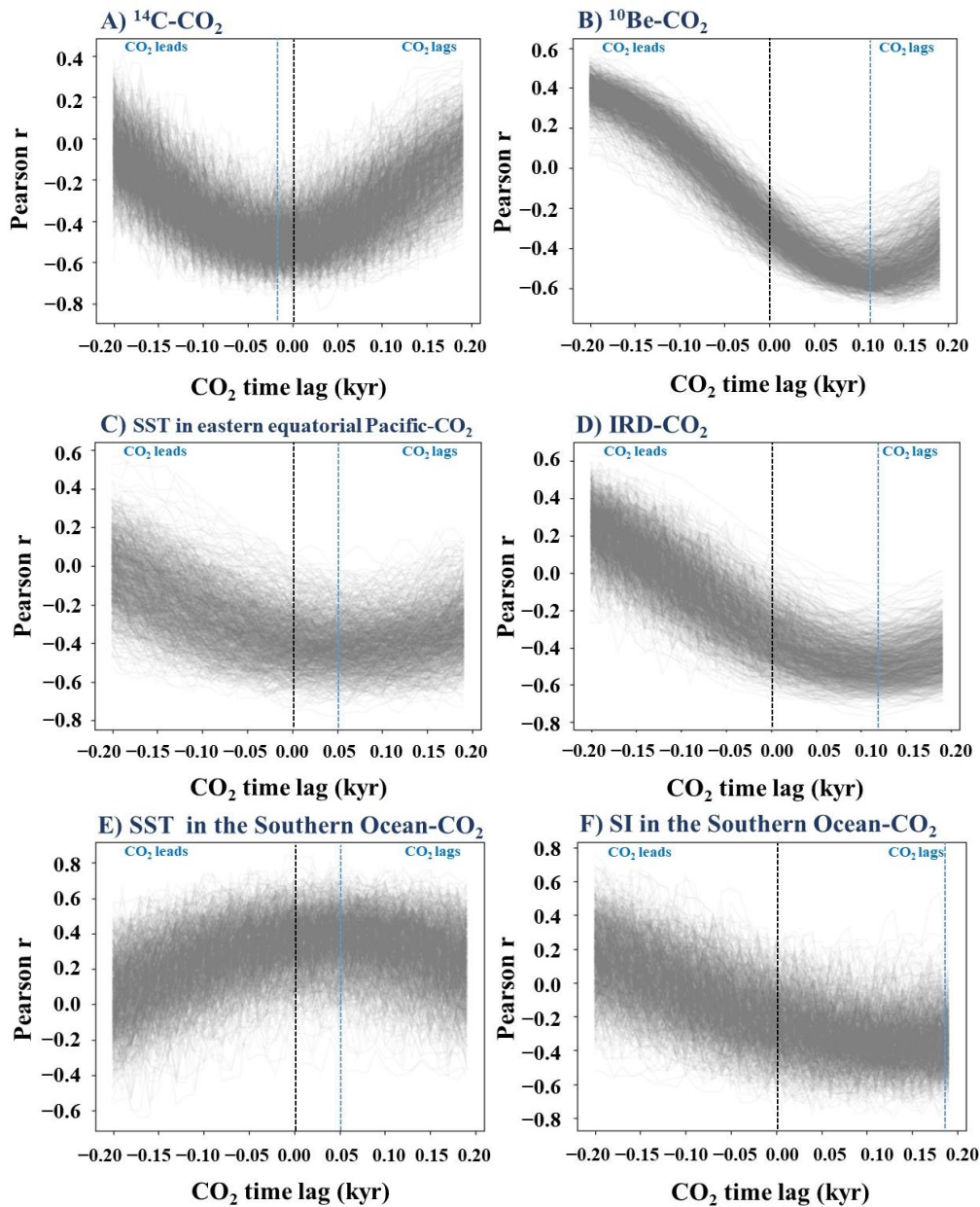


Figure 4. Correlation coefficients between CO₂ and proxies with CO₂ time lag calculated from Monte Carlo simulation. Vertical lines in black indicate zero time lag. Vertical lines in blue indicate maximum correlation coefficients between CO₂ and proxies with CO₂ time lag. A) ¹⁴C production rate and atmospheric CO₂. B) ¹⁰Be flux and atmospheric CO₂. C) SST in the eastern equatorial Pacific and atmospheric CO₂. D) IRD from the North Atlantic and atmospheric ~~CO₂~~ CO₂. E) SST in the East Equatorial Pacific indicating El Niño-like or La Niña-like conditions and atmospheric CO₂. F) SI in the East Equatorial Pacific and atmospheric CO₂.

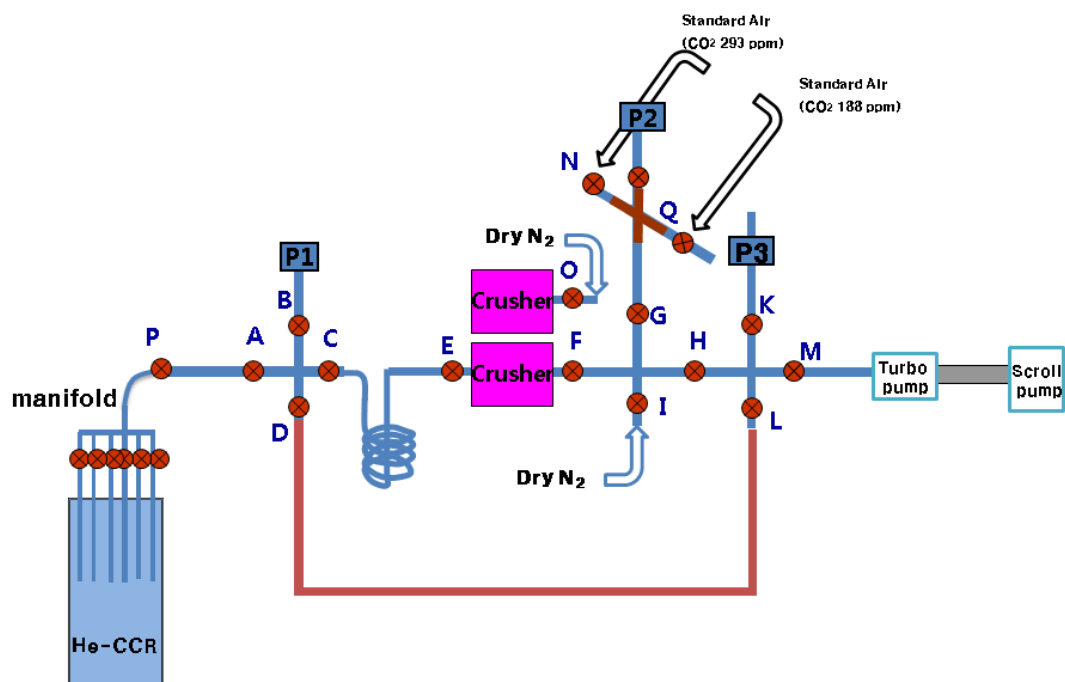


Figure S1. Schematic diagram of the dry extraction system used for this study. Details are described in Ahn et al. (2009). He-CCR stands for He-Closed Cycled Refrigerator.

5

10

15

Table S1. Comparison of CO₂ analysis with two different standard airs (188.9 and 293.3 ppm) in order to check the linearity in the gas chromatograph.

Siple Dome ice core	With 188.9 ppm Standard air				With 293.3 ppm Standard air				Difference	
Mean depth (m)	CO ₂ (ppm)	mean CO ₂ (ppm)	uncertainty (ppm)	# of samples	CO ₂ (ppm)	mean CO ₂ (ppm)	uncertainty (ppm)	# of samples	CO ₂ (ppm)	uncertainty (ppm)
640.53	248.7	249.6	0.9	2	250.7	249.6	0.9	3	0.0	1.3
	250.5				247.8					
644.22	246.0	246.0	0.1	2	247.8	247.2	0.6	2	1.2	0.6
	246.1				246.6					
668.09	241.7	242.2	0.5	2	242.3	243.1	0.8	2	0.9	0.9
	242.7				243.8					
671.51	243.7	243.0	0.7	2	242.8	243.5	0.4	3	0.5	0.8
	242.3				243.5					
673.47	241.1	240.4	0.8	2	239.1	239.8	0.7	2	-0.6	1.0
	239.6				240.5					
Average									0.4	0.9

Table S2. Interlaboratory comparison between SNU (Seoul National University) and OSU (Oregon State University) using Siple Dome ice core.

Depth range (m)	SNU CO ₂ (ppm)	# of replicates	OSU CO ₂ (ppm)	#of replicates	SNU-OSU (ppm)
490.17–490.22	266.8	2	265.7	3	1.1
500.40–500.45	263.8	2	264.1	4	-0.3
501.87–502.41	263.8	2	262.8	2	1.1
506.60–506.65	264.9	3	265.0	2	-0.1
522.90–523.10	266.7	2	266.3	2	0.5
523.28–523.33	265.2	2	265.8	2	-0.6
530.50–530.55	266.9	2	266.4	2	0.6
Average					0.3
Standard deviation					0.7

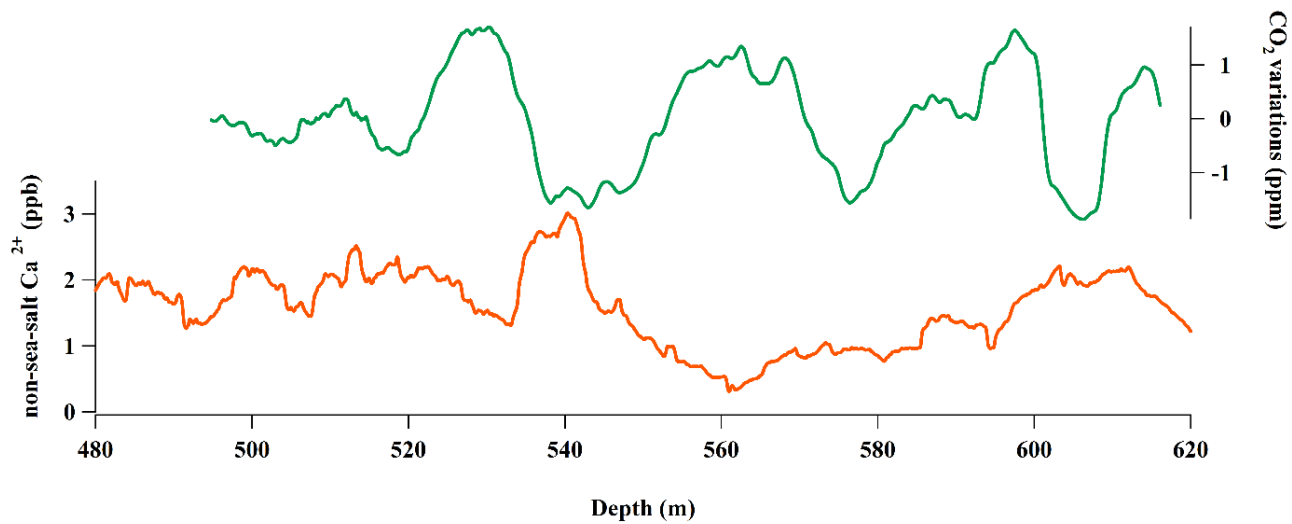


Figure S2. Comparison of Siple Dome millennial (filtered) CO₂ record (Ahn et al., 2014) and non-sea-salt Ca²⁺ on depth domain. The non-sea-salt Ca²⁺ data are 250-yr running means.

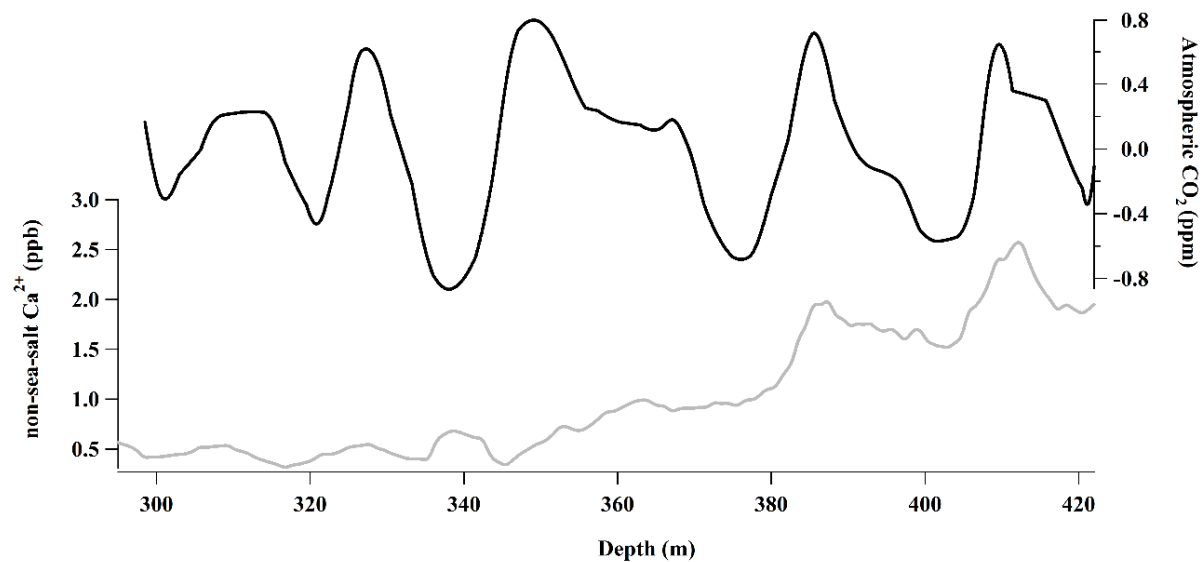


Figure S3. Comparison of Dome C millennial (filtered) CO₂ record (Monnin et al., 2001; Monnin et al., 2004) and non-sea-salt Ca²⁺ (Lambert et al., 2012) on depth domain. The non-sea-salt Ca²⁺ data are 250-yr running means.

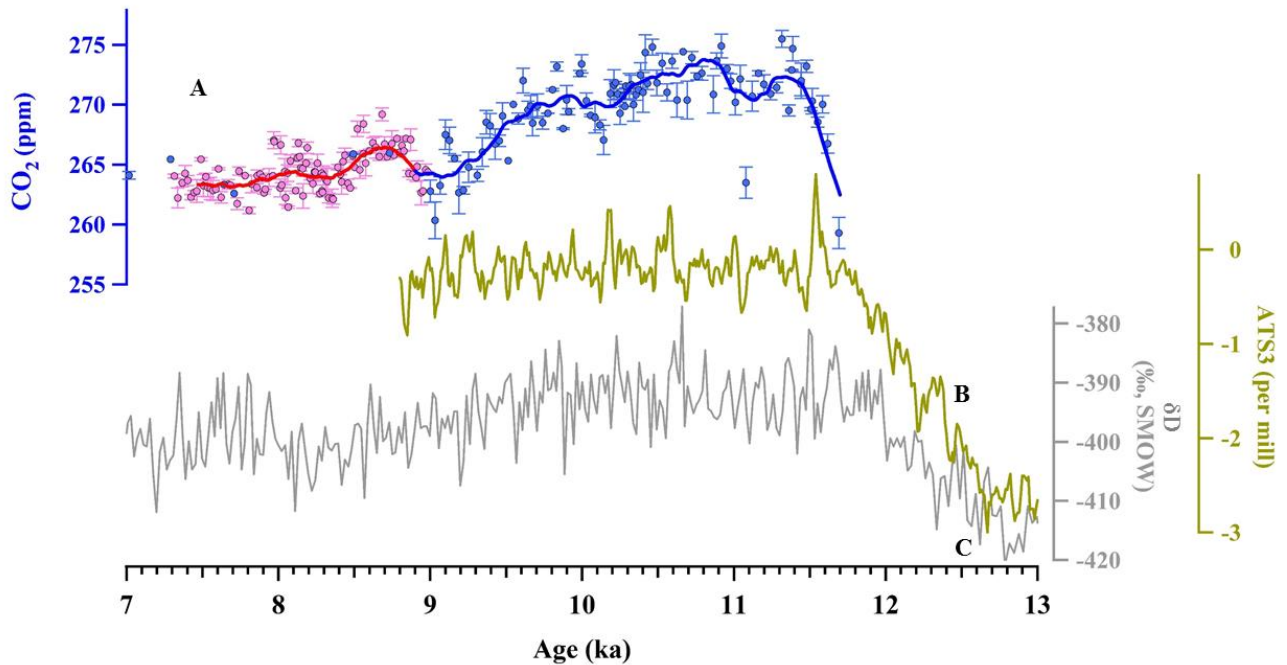


Figure S4. High-resolution atmospheric CO₂ records obtained from Siple Dome ice core, Antarctica during the early Holocene. A) Pink and blue circles are Siple Dome ice core records obtained at OSU (Ahn et al., 2014) and SNU (this study), respectively. Lines in pink and blue represent 250-yr running means. B) Antarctic temperature Stack 3 (ATS3) developed by Buizert et al. (2018) using five records: Dome C, Dome Fuji, Talos Dome, EPICA Dronning Maud Land and WAIS Divide. C) Grey line indicates δD in the Dome C ice core, Antarctica (Jouzel et al., 2007).

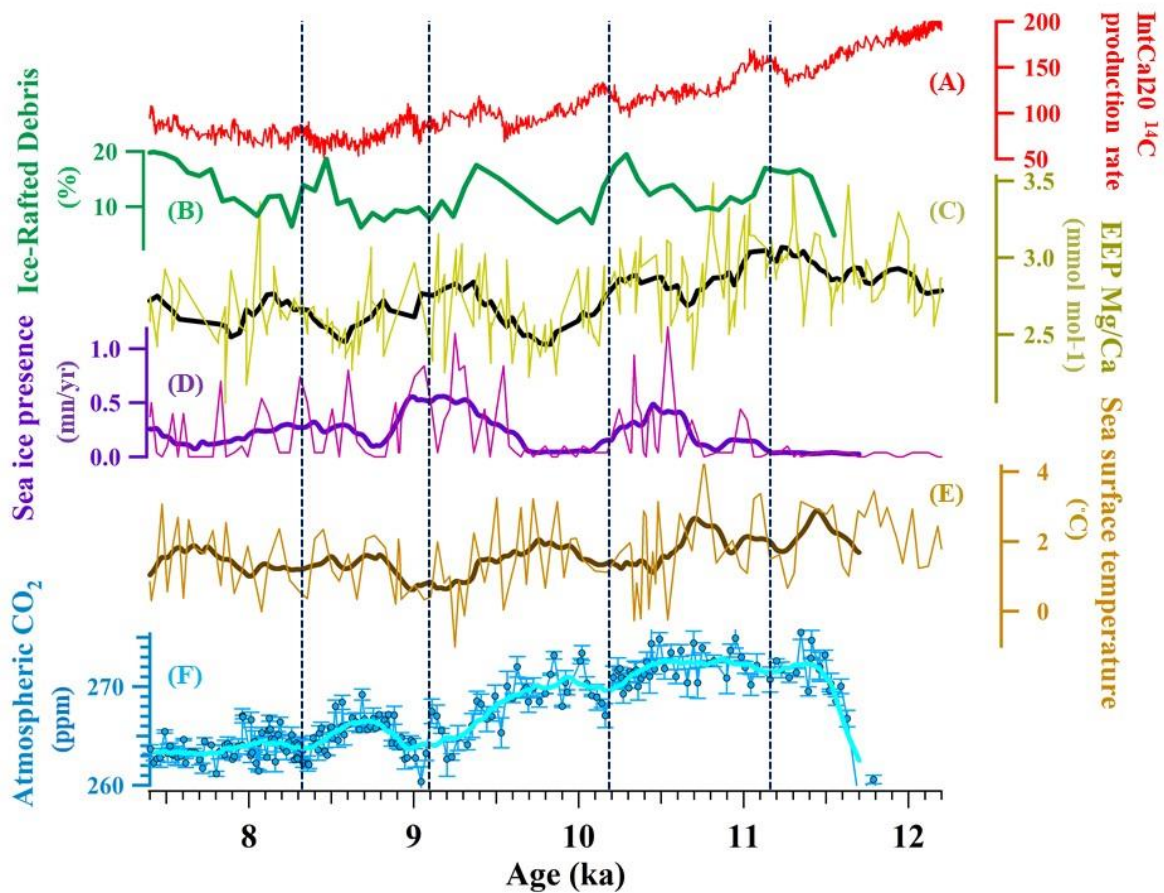


Figure S5. Comparison of atmospheric CO₂ with climatic proxy records over the early Holocene. Lines represent 250-yr running means. (A) IntCal20¹⁴C production rate (Reimer et al., 2020). (B) Ice rafted debris stacked records from the North Atlantic regions on untuned calibrated ¹⁴C age model (Bond et al., 2001; Marchitto et al., 2010). (C) Sea surface temperature from the eastern equatorial Pacific indicating El Niño-like or La Niña-like conditions (Marchitto et al., 2010). (D) Sea ice presence from the Polar Front of the Southern Ocean on the chronology of Mortyn et al. (2003) (Nielsen et al., 2004). (E) Sea surface temperature from the Polar Front of the Southern Ocean on the chronology of Mortyn et al. (2003) (Nielsen et al., 2004). (F) Atmospheric CO₂ record from Siple Dome (in this study).

Monte Carlo simulation

We calculate uncertainties of a smoothed CO₂ record by using Monte Carlo simulation (Figure 1). Random sampling was made from a probability distribution for each measured value and its standard deviation. We repeated this series of simulations 10,000 times, which is shown as 2σ in Figure 1

5 The uncertainty band is narrow, which is attributed to the removal of the high frequency signal by 250-yr running means. When the Monte Carlo simulation was conducted, we considered that each data follows a normal distribution. The width of the error band is affected by neighbouring data points. If the data points are close together, the error of neighbouring data points in the opposite direction can be canceled out, resulting in a narrow uncertainty band.

We evaluated 250-yr running means and their uncertainties by using a new Monte Carlo approach. Random sampling was made from a probability distribution for each measured value and its standard deviation. If the standard deviation was smaller than the average reproducibility of the measurement ($1\sigma = 0.87$ ppm), we used 0.87 ppm as the uncertainty of a measured value. Then, 1-yr interpolation and resampling were applied to generate an evenly-spaced time series and to calculate the 250-yr running means. We repeated this series of simulations 10,000 times and evaluated the mean of 250-yr running means and its uncertainty (shown as 2σ in Figure S6). We used a modified Akima method using the built-in makima function in Matlab
15 for the interpolation. The different types of interpolation and smoothing methods resulted in insignificant differences in the 250-yr running means.

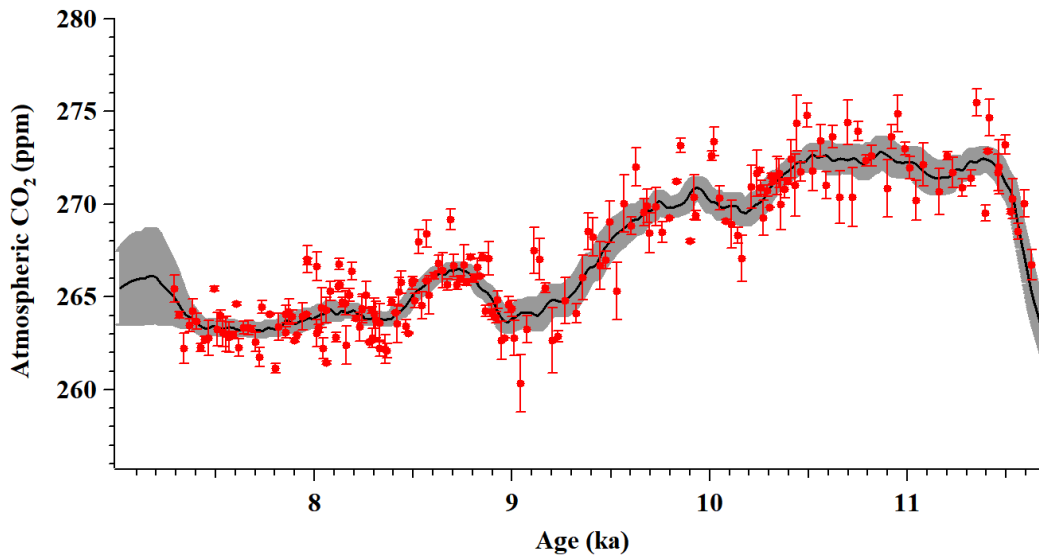


Figure S6. Red circles are Siple Dome ice core records during the early Holocene (11.7–7.4 ka). The black line indicates the average of 10,000 times modified akima simulations showing an error-weighted average of the CO₂ record. The dark shaded indicates 2σ uncertainties calculated from modified akima simulations.

Correlation coefficients between CO₂ and climate proxies

In order to assess the relationship between CO₂ and climate, we calculate correlations and estimate leads and lags between CO₂ and proxies of solar activity as well as climate proxies thought to be themselves related to solar activity. The Pearson correlation coefficient r is commonly used to verify relationships between variables. However, r does not take chronological uncertainty into account. As such, we apply a Monte Carlo procedure to estimate the correlations between CO₂ and climate proxies. In the procedure, we adjust the chronologies of the two series, within their chronological uncertainties, and re-calculate r . We do so 1,000 times for each pair, allowing us to calculate a mean correlation coefficient that is more representative of the relationship between time-uncertain series.

We use a similar method to calculate the significance of this correlation against a random red-noise process. At each of the 1,000 steps, we use an AR(1) model (lag-1 auto regression) to fit data series. We then use these AR(1) characteristics to randomly generate two synthetic series with the same red noise. Then, we calculate the percentage of correlations between the randomized synthetic series that are lower than the correlation coefficients of the real series to assess the significance of the correlation.

Finally, we can calculate the maximum-correlation lag between the two series. At each step in the 1,000 iteration Monte Carlo procedure, we calculate the lag which gives the maximum correlation by shifting one of the series by 10-yr increments, for constant lags between -200 (a CO₂ lead) and 200 yrs (a CO₂ lag). Then, we make a histogram of the calculated maximum-correlation lags, from which the mode can be selected as an approximation of the phasing between the two series. We also report the maximum correlation between the two series, but note that this is not representative of the actual relationship (it simply gives an idea of how much the correlation can be improved by adding a lag between the two series).

20

25

30

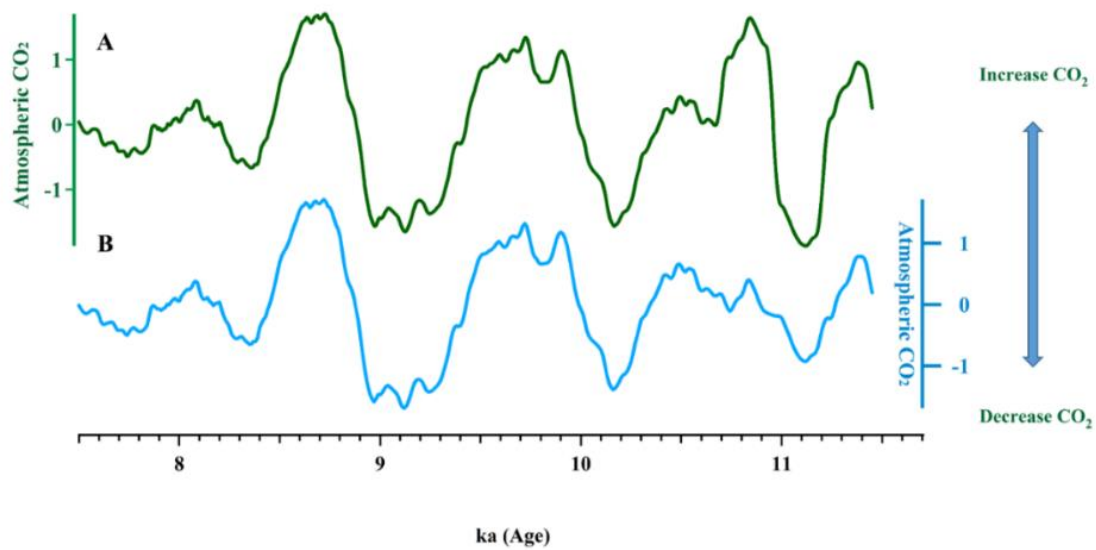


Figure S76. (A) Green line indicates CO₂ original data which was filtered by high pass filtering. (B) Blue line indicates CO₂ data filtered by high pass filtering without 2 points at 11.8 ka and 10.825 ka.

Table S3. Correlation between Siple Dome CO₂ record without single outliers at 10.8 ka and 11.1 ka and climate proxy records. Column A shows correlation coefficients between CO₂ and proxies with CO₂ time lags. Column B shows correlation coefficients between CO₂ and proxies without CO₂ time lag. “With MC” are mean values from the simulations taking age uncertainties into account. “Without MC” is the classic calculation of correlation, without taking age uncertainty into account. Significance of the lag correlations was assessed against 1,000 repetitions of the lag correlation calculation using synthetic data stochastically generated to have the same red noise characteristics as the original series.

<u>Proxy records</u>	<u>A: Correlation between CO₂ and proxies with CO₂ time lag (yrs)</u>				<u>B: Correlation between CO₂ and proxies without CO₂ time lag</u>	
	<u>With MC</u>		<u>Without MC</u>		<u>With MC</u>	<u>Without MC</u>
	<u>r (p-value)</u>	<u>Time lag</u>	<u>r (p-value)</u>	<u>Time lag</u>	<u>r (p-value)</u>	<u>r (p-value)</u>
<u>CO₂ - ¹⁴C production rate</u> <u>Marchitto et al.(2010);</u> <u>Reimer et al.(2004)</u>	<u>-0.44±0.10</u> <u>(0.010)</u>	<u>0±148</u>	<u>-0.76</u> <u>(<0.001)</u>	<u>40</u>	<u>-0.43</u> <u>(0.005)</u>	<u>-0.62</u> <u>(<0.001)</u>
<u>CO₂ - ¹⁰Be flux from Greenland ice core</u> <u>Finkel and Nishiizumi (1997);</u> <u>Marchitto et al. (2010);</u> <u>Vonmoos et al. (2006)</u>	<u>-0.30±0.06</u> <u>(0.101)</u>	<u>130±63</u>	<u>-0.58</u> <u>(<0.001)</u>	<u>120</u>	<u>-0.30</u> <u>(0.021)</u>	<u>-0.36</u> <u>(<0.001)</u>
<u>CO₂ - IRD from the North Atlantic region</u> <u>Bond et al. (2001);</u> <u>Marchitto et al. (2010)</u>	<u>-0.44±0.11</u> <u>(0.076)</u>	<u>70±155</u>	<u>-0.73</u> <u>(<0.001)</u>	<u>160</u>	<u>-0.32</u> <u>(0.057)</u>	<u>-0.23</u> <u>(0.001)</u>
<u>CO₂ - SST from eastern equatorial Pacific</u> <u>Marchitto et al. (2010)</u>	<u>-0.37±0.13</u> <u>(0.057)</u>	<u>0±219</u>	<u>-0.61</u> <u>(<0.001)</u>	<u>80</u>	<u>-0.34</u> <u>(0.044)</u>	<u>-0.56</u> <u>(<0.001)</u>
<u>CO₂ - Sea ice in the Southern Ocean</u> <u>Nielsen et al. (2004)</u>	<u>-0.32±0.16</u> <u>(0.171)</u>	<u>-</u> <u>180±22</u> <u>8</u>	<u>-0.57</u> <u>(<0.001)</u>	<u>80</u>	<u>-0.24</u> <u>(0.155)</u>	<u>-0.49</u> <u>(<0.001)</u>
<u>CO₂ - SST in the Southern Ocean</u> <u>Nielsen et al. (2004)</u>	<u>0.35±0.16</u> <u>(0.075)</u>	<u>60±228</u>	<u>0.58</u> <u>(<0.001)</u>	<u>20</u>	<u>0.35</u> <u>(0.063)</u>	<u>0.58</u> <u>(<0.001)</u>
<u>CO₂ - NGRIP δ¹⁸O</u> <u>Rasmussen et al. (2006)</u>	<u>0.18±0.06</u> <u>(0.180)</u>	<u>-</u> <u>140±63</u>	<u>0.20</u> <u>(0.080)</u>	<u>-110</u>	<u>0.17</u> <u>(0.180)</u>	<u>0.16</u> <u>(0.001)</u>

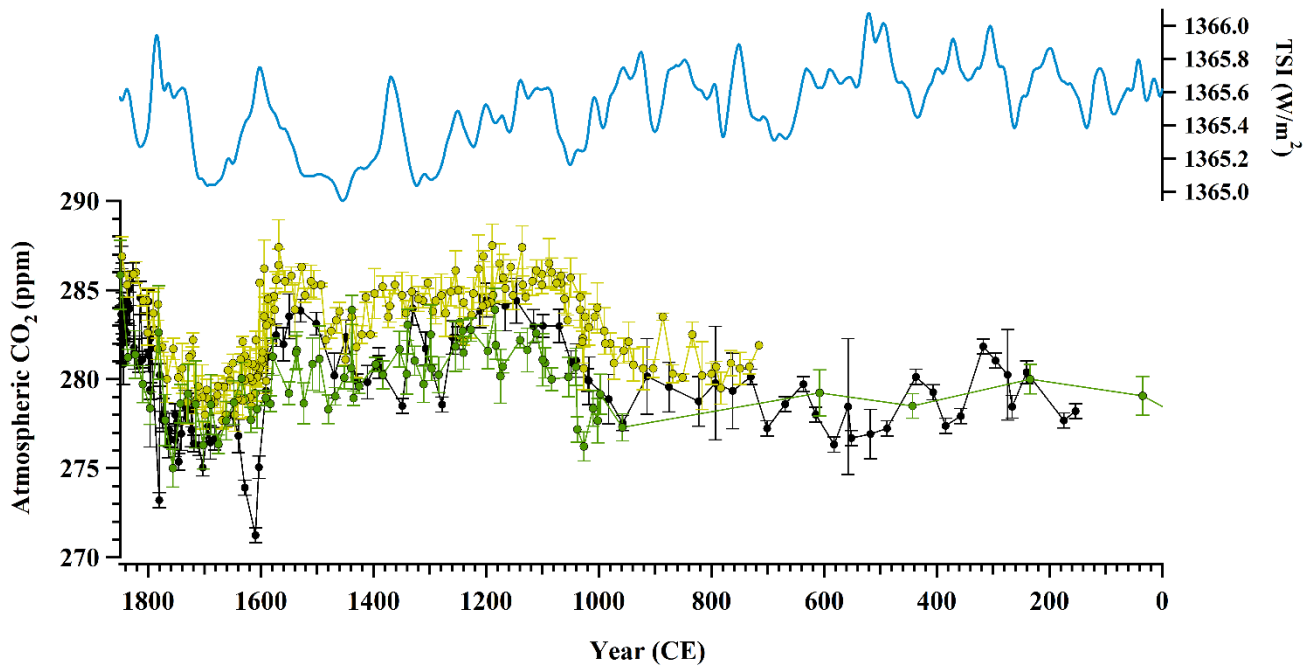


Figure S8. Atmospheric CO₂ from Antarctic ice cores during the last 2,000 yrs. Blue line: total solar irradiance (TSI) (Roth and Joos, 2013). Yellow dots: atmospheric CO₂ from WAIS Divide ice core (Ahn et al., 2012). Green dots: atmospheric CO₂ from EPICA Dronning Maud Land (EDML) (Monnin et al., 2004; Siegenthaler et al., 2005). Black dots: atmospheric CO₂ from Law Dome (Rubino et al., 2019).

References

- Ahn, J., Brook, E. J., and Buizert, C.: Response of atmospheric CO₂ to the abrupt cooling event 8200 years ago, *Geophys. Res. Lett.*, 41, 604–609, <https://doi.org/10.1002/2013gl058177>, 2014.
- Ahn, J., Brook, E. J., Mitchell, L., Rosen, J., McConnell, J. R., Taylor, K., Etheridge, D., and Rubino, M.: Atmospheric CO₂ over the last 1000 years: A high-resolution record from the West Antarctic Ice Sheet (WAIS) Divide ice core, *Global Biogeochem. Cy.*, 26, GB2027, <https://doi.org/10.1029/2011GB004247>, 2012.
- Ahn, J. H., Brook, E. J., and Howell, K.: A high-precision method for measurement of paleoatmospheric CO₂ in small polar ice samples, *J. Glaciol.*, 55, 499–506, 2009.
- Bond, G., Kromer, B., Beer, J., Muscheler, R., Evans, M. N., Showers, W., Hoffmann, S., Lotti-Bond, R., Hajdas, I., and Bonani, G.: Persistent solar influence on North Atlantic climate during the Holocene, *Science*, 294, 2130–2136, 2001.
- Buizert, C., Sigl, M., Severi, M., Markle, B. R., Wettstein, J. J., McConnell, J. R., Pedro, J. B., Sodemann, H., Goto-Azuma, K., Kawamura, K., et al.: Abrupt ice-age shifts in southern westerly winds and Antarctic climate forced from the north, *Nature*, 563, 681–685, 2018.
- [Finkel, R. C. and Nishiizumi, K.: Beryllium 10 concentrations in the Greenland Ice Sheet Project 2 ice core from 3–40 ka, *J. Geophys. Res.*, 102\(C12\), 26699–26706, doi:199710.1029/97JC01282, 1997.](https://doi.org/10.1029/1997JC01282)
- Jouzel, J., Masson-Delmotte, V., Cattani, O., Dreyfus, G., Falourd, S., Hoffmann, G., Minster, B., Nouet, J., Barnola, J. M., Chappellaz, J., Fischer, H., Gallet, J. C., Johnsen, S., Leuenberger, M., Loulergue, L., Luethi, D., Oerter, H., Parrenin, F., Raisbeck, G., Raynaud, D., Schilt, A., Schwander, A., Selmo, E., Souchez, R., Spahni, R., Stauffer, B., Steffensen, J. P., Stenni, B., Stocker, T.F., Tison, J. L., Werner, M., and Wolff, E. W.: Orbital and Millennial Antarctic Climate Variability over the Past 800,000 Years, *Science*, 317, 793–796, <https://doi.org/10.1126/science.1141038>, 2007.
- Lambert, F., Bigler, M., Steffensen, J. P., Hutterli, M., and Fischer, H.: Centennial mineral dust variability in high-resolution ice core data from Dome C, Antarctica, *Clim. Past*, 8, 609–623, <https://doi.org/10.5194/cp-8-609-2012>, 2012.
- Marchitto, T. M., Muscheler, R., Ortiz, J. D., Carriquiry, J. D., and van Geen, A.: Dynamical response of the tropical Pacific Ocean to solar forcing during the early Holocene, *Science*, 330, 1378–1381, 2010.
- Monnin, E., Steig, E. J., Siegenthaler, U., Kawamura, K., Schwander, J., Stauffer, B., Stocker, T. F., Morse, D. C., Barnola, J.-M., Bellier, B., Raynaud, D., and Fischer, H.: Evidence for substantial accumulation rate variability in Antarctica during the Holocene through synchronization of CO₂ in the Taylor Dome, Dome C and DML ice cores, *Earth Planet. Sc. Lett.*, 224, 45–54, 2004.
- Monnin, E., Indermuhle, A., Dallenbach, A., Fluckiger, J., Stauffer, B., Stocker, T. F., Raynaud, D., and Barnola, J.-M.: Atmospheric CO₂ concentrations over the last glacial termination, *Science*, 291(5501), 112–114, 2001.
- Mortyn, P. G., Charles, C. D., Ninnemann, U. S., Ludwig, K., and Hodell, D. A.: Deep sea sedimentary analogues for the Vostok ice core, *Geochem. Geophys. Geosy.*, 4, 8405, doi:10.1029/2002GC000475, 2003.

- Nielsen, S. H. H., Koc, N., and Crosta, X.: Holocene climate in the Atlantic sector of the southern ocean: Controlled by insolation or oceanic circulation?, *Geology*, 32, 317–320, 2004.
- [Rasmussen, S. O., Andersen, K. K., Svensson, A. M., Steffensen, J. P., Vinther, B. M., Clausen, H. B., Siggaard-Andersen, M.-L., Johnsen, S. J., Larsen, L. B., Dahl-Jensen, D., Bigler, M., Rothlisberger, R., Fischer, H., Goto-Azuma, K., Hansson, M.E., and Ruth, U.: A new Greenland ice core chronology for the last glacial termination, *J. Geophys. Res.*, 111, D06102, <https://doi.org/10.1029/2005JD006079>, 2006.](#)
- 5 [Reimer, P. J., Austin, W. E. N., Bard, E., Bayliss, A., Blackwell, P. G., Ramsey, C. B., Butzin, M., Cheng, H., Edwards, R. L., Friedrich, M., Grootes, P. M., Guilderson, T. P., Hajdas, I., Heaton, T. J., Hogg, A. G., Hughen, K. A., Kromer, B., Manning, S. W., Muscheler, R., Palmer, J. G., Pearson, C., van der Plicht, J., Reimer, R. W., Richards, D. A., Scott, E. M., Southon, J.](#)
- 10 [R., Turney, C. S. M., Wacker, L., Adolphi, F., Büntgen, U., Capano, M., Fahrni, S. M., Fogtmann-Schulz, A., Friedrich, R., Köhler, P., Kudsk, S., Miyake, F., Olsen, J., Reinig, F., Sakamoto, M., Sookdeo, A., and Talamo, S.: The IntCal20 Northern Hemisphere radiocarbon age calibration curve \(0–55 cal. ka BP\), *Radiocarbon*, 62, 725–757, <https://doi.org/10.1017/RDC.2020.41>, 2020.](#)
- [Reimer, P. J., Baillie, M. G., Bard, E., Beck, J. W., Buck, C. E., Blackwell, P. G., Burr, G. S., Cutler, K. B., Damon, P. E.,](#)
- 15 [Edwards, R. L., Fairbanks, R. G., Friedrich, M., Guilderson, T. P., Hogg, A. G., Hughen, K. A., Kromer, B., McCormac, G., Ramsey, C. B., Reimer, R. W., Remmele, S., Southon, J. R., Stuiver, M., Taylor, F. W., van der Plicht, J., and Weyhenmeyer, C. E.: IntCal04: A New Consensus Radiocarbon Calibration Dataset from 0–26 ka BP, *Radiocarbon*, 46, 1029–1058, 2004.](#)
- Roth, R. and Joos, F.: A reconstruction of radiocarbon production and total solar irradiance from the Holocene ^{14}C and CO_2
- 20 records: implications of data and model uncertainties, *Clim. Past*, 9, 1879–1909, <https://doi.org/10.5194/cp-9-1879-2013>, 2013.
- Rubino, M., Etheridge, D. M., Thornton, D. P., Howden, R., Allison, C. E., Francey, R. J., Langenfelds, R. L., Steele, L. P., Trudinger, C. M., Spencer, D. A., Curran, M. A. J., van Ommen, T. D., and Smith, A. M.: Revised records of atmospheric trace gases CO_2 , CH_4 , N_2O , and $\delta^{13}\text{C}\text{-CO}_2$ over the last 2000 years from Law Dome, Antarctica, *Earth Syst. Sci. Data*, 11, 473–492, <https://doi.org/10.5194/essd-11-473-2019>, 2019.
- 25 [Siegenthaler, U., Monnin, E., Kawamura, K., Spahni, R., Schwander, J., Stauffer, B., Stocker, T. F., Barnola, J.-M., and Fischer, H.: Supporting evidence from the EPICA Dronning Maud Land ice core for atmospheric \$\text{CO}_2\$ changes during the past millennium, *Tellus B*, 57\(7\), 51–57, doi:10.1111/j.1600- 0889.2005.00131.x, 2005.](#)
- [Vonmoos, M., Beer, J., and Muscheler, R.: Large variations in Holocene solar activity: Constraints from \$^{10}\text{Be}\$ in the Greenland Ice Core Project ice core, *J. Geophys. Res.-Space*, 111, A10105, doi:10.1029/2005JA011500, 2006.](#)
- 30 [Bond, G., Kromer, B., Beer, J., Muscheler, R., Evans, M. N., Showers, W., Hoffmann, S., Lotti-Bond, R., Hajdas, I., and Bonani, G.: Persistent solar influence on North Atlantic climate during the Holocene, *Science*, 294, 2130–2136, 2001.](#)